

Information Theoretic Evaluation of Privacy-Leakage, Interpretability, and Transferability for a Novel Trustworthy AI Framework*

Mohit Kumar^{a,b,*}, Bernhard A. Moser^a, Lukas Fischer^a, Bernhard Freudenthaler^a

^aSoftware Competence Center Hagenberg GmbH, A-4232 Hagenberg, Austria.

^bFaculty of Computer Science and Electrical Engineering, University of Rostock, Germany.

Abstract

Guidelines and principles of trustworthy AI should be adhered to in practice during the development of AI systems. This work suggests a novel information theoretic trustworthy AI framework based on the hypothesis that information theory enables taking into account the ethical AI principles during the development of machine learning and deep learning models via providing a way to study and optimize the inherent tradeoffs between trustworthy AI principles. A unified approach to “privacy-preserving interpretable and transferable learning” is presented via introducing the information theoretic measures for privacy-leakage, interpretability, and transferability. A technique based on variational optimization, employing conditionally deep autoencoders, is developed for practically calculating the defined information theoretic measures for privacy-leakage, interpretability, and transferability.

Keywords: Trustworthy AI, privacy, interpretability, transfer learning, information theory, machine and deep learning.

1. Introduction

Trust in the development, deployment, and use of AI is essential to fully utilize the AI-potential in contributing to human well being and society. The recent advances in machine and deep learning have rejuvenated the field of AI with an enthusiasm that AI would become an integral part of human life. However, rapid proliferation of AI will give rise to several ethical, legal, and social issues.

1.1. Trustworthy AI and Guidelines

In response to the ethical, legal, and social challenges accompanied by AI, guidelines and ethical principles have been established [6, 1, 2, 3] to evaluate the responsible development of AI systems that are good for humanity and the environment. The guidelines have introduced the concept of *trustworthy AI* (TAI) and the term TAI has quickly gained attention in research and practice. TAI is based on the idea that trust in AI will make AI realize its full potential in contributing to societies, economies, and sustainable development. As “trust” is a complex phenomenon being studied in diverse disciplines (i.e. psychology, sociology, economics, management, computer science, and information systems), the definition and realization of TAI remains challenging. While forming trust in technology, users express expectations about the technology’s *functionality*, *helpfulness* and *reliability* [17]. The authors in [21] state that “*AI is perceived as trustworthy*

*The research reported in this paper has been supported by the Austrian Research Promotion Agency (FFG) Sub-Project PETAI (Privacy Secured Explainable and Transferable AI for Healthcare Systems); the Federal Ministry for Climate Action, Environment, Energy, Mobility, Innovation and Technology (BMK); the Federal Ministry for Digital and Economic Affairs (BMDW); and the Province of Upper Austria in the frame of the COMET - Competence Centers for Excellent Technologies Programme managed by Austrian Research Promotion Agency FFG.

*Corresponding author

Email address: mohit.kumar@uni-rostock.de, mohit.kumar@scch.at (Mohit Kumar)

by its users (e.g., consumers, organizations, society) when it is developed, deployed, and used in ways that not only ensure its compliance with all relevant laws and its robustness but especially its adherence to general ethical principles”.

Academicians, industries, and policymakers have developed in recent times for TAI several frameworks and guidelines including “Asilomar AI Principles” [4], “Montreal Declaration of Responsible AI” [23], “UK AI Code” [22], “AI4People” [3], “Ethics Guidelines for Trustworthy AI” [6], “OECD Principles on AI” [19], “Governance Principles for the New Generation Artificial Intelligence” [18], and “Guidance for Regulation of Artificial Intelligence Applications” [24]. However, it was argued in [5] that AI ethics lack a reinforcement mechanism and economic incentives could easily override commitment to ethical principles and values.

1.2. Principles of Ethical AI

The five principles of ethical AI [3] (i.e. *beneficence, non-maleficence, autonomy, justice, and explicability*) have been adopted for TAI [21]. Beneficence refers to promoting well-being of humans, preserving dignity, and sustaining the planet. Non-maleficence refers to avoiding bringing harm to people and is especially concerned with the protection of people’s privacy and security. Autonomy refers to the promotion of human autonomy, agency, and oversight including the restriction of AI Systems’ autonomy, where necessary. Justice refers to using AI for correcting past wrongs, ensuring shared benefits through AI; and preventing the creation of new harms and inequities by AI. Explicability comprises an epistemological sense and an ethical sense. Explicability refers in epistemological sense to the explainable AI via creating interpretable AI models with high levels of performance and accuracy. In ethical sense, explicability refers to accountable AI. Despite the importance of outlined TAI principles, their major limitation, as identified in [21], is concerning the fact that principles are highly general and provide little to no guidance for how they can be transferred into practice. To address this limitation, a data-driven research framework for TAI was outlined in [21].

1.3. Motivation of the Current Study

We identify in Table 1 the core issues related to machine learning and deep learning based AI systems that need to be addressed for fulfilling the five principles of trustworthy AI. The solution approaches to address the issues concerning TAI (as identified in Table 1) do exist in the literature, however, a unified solution approach addressing all major issues doesn’t exist. Thus, the motivation of this study is derived from the requirement of a TAI framework addressing the core issues in a rigorous analytical manner.

1.4. Proposed Framework for Trustworthy AI

We hypothesize that an information theoretic unified approach leads to the development of a framework allowing transferring of TAI principles into practice. We propose a novel framework, referred to as *Information Theoretic Trustworthy Artificial Intelligence* (ITTAI), for the design and analysis of trustworthy AI systems. The ITTAI framework is based on the hypothesis that *information theory enables taking into account the trustworthy AI principles of beneficence, non-maleficence, autonomy, justice, and explicability during the development of machine learning and deep learning based AI systems via providing a way to study and optimize the inherent tradeoffs between TAI principles*. The overall aim of ITTAI framework is to facilitate transfer of TAI principles into practice via fulfilling following aims:

- Aim 1:** To develop an information theoretic approach to privacy enabling the quantification of privacy leakage in-terms of mutual information between sensitive private data and the released public data without the availability of a prior knowledge about data statistics (such as joint distributions of public and private variables).
- Aim 2:** To develop an information theoretic criterion for evaluating the interpretability of a machine learning model in-terms of mutual information between non-interpretable model outputs/activations and corresponding interpretable parameters.
- Aim 3:** To develop an information theoretic criterion for evaluating the transferability (of a machine learning model from source to target domain) in-terms of mutual information between source domain model outputs/activations and target domain model outputs/activations.

Table 1: Core issues of TAI principles and solution approach

TAI principle	issue	solution approach
Beneficence	I1: non-availability of large high-quality training data	transfer learning
	I2: models (intellectual properties) are not widely available	federated learning
Non-maleficence	I3: leakage of private information embedded in training data	privacy-preserving data release mechanism
	I4: leakage of private information embedded in model parameters and model outputs	privacy-preserving machine and deep learning
Autonomy	I5: user’s inability to quantify model-uncertainties leads to indecisiveness regarding the level of autonomy given to AI system	analytical quantification of model uncertainties
Justice	I6: bias of training data towards certain groups of people leads to discrimination	federated learning
Explicability	I7: user’s inability to understand model functionality leads to mistrust and obstruction in establishing accountability	interpretable machine and deep learning models

Aim 4: To develop analytical approaches to machine and deep learning allowing quantification of model uncertainties.

Aim 5: To develop a unified approach to “privacy-preserving interpretable and transferable learning” for an analytical optimization of privacy-interpretability-transferability tradeoffs.

ITTAI framework (with its structure as in Fig. 1) addresses the

1. issues **I1** and **I2** of beneficence principle by means of transfer and federated learning;
2. issues **I3** and **I4** of non-maleficence principle by means of privacy-preserving data release mechanisms;
3. issue **I5** of autonomy principle by means of analytical machine and deep learning algorithms enabling the user to quantify model uncertainties and hence to decide the level of autonomy given to AI systems;
4. issue **I6** of justice principle by means of federated learning;
5. issue **I7** of explicability principle by means of interpretable machine and deep learning models.

The most important feature of ITTAI is that the notions of privacy, interpretability, and transferability are quantified by means of information theoretic measures allowing the study and optimization of tradeoffs between TAI principles (such as tradeoff between privacy and transferability, or tradeoff between privacy and interpretability) in a practical manner.

1.5. Novelty and Contributions

This study presents a unified approach to “privacy-preserving interpretable and transferable learning” under the proposed ITTAI framework. The study introduces the information theoretic measures for privacy-leakage, interpretability, and transferability. It is possible to derive analytical expressions for the defined measures, provided a knowledge regarding the statistical data distributions is available. However, in practice,

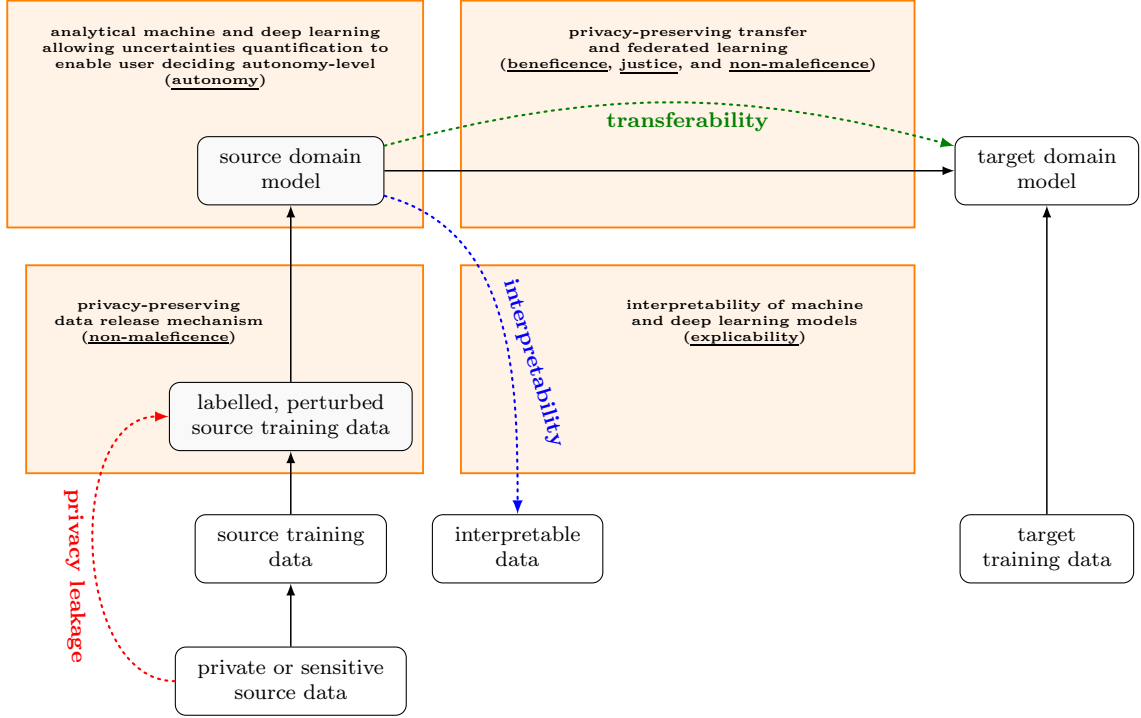


Figure 1: ITTAI framework facilitates a transfer of TAI principles (beneficence, non-maleficence, autonomy, justice, and explicability) into practice via providing an information theoretic unified approach to “privacy-preserving interpretable and transferable learning” for studying the privacy-interpretability-transferability tradeoffs.

the data distributions are unknown and thus a way to approximate the defined measures is required. Therefore, a novel method, that employs recently introduced conditionally deep autoencoders [10], is presented for approximating the defined privacy-leakage, interpretability, and transferability measures. The method relies on inferring a variational Bayesian inverse model that facilitates an analytical approximation of the information theoretic measures through variational optimization methodology. Finally, a computational algorithm is provided for practically calculating the privacy-leakage, interpretability, and transferability measures.

1.6. Contents and Organization

This text is organized into sections. The proposed methodology in this study relies heavily on the Bregman divergence based conditionally deep autoencoders for data representation learning. Therefore, section 2 has been dedicated to the review of conditionally deep autoencoders from [10]. Under the proposed ITTAI framework, we adopt the transfer learning approach of [7] that combines conditionally deep autoencoder with a tailored noise adding mechanism to achieve a given level of privacy-loss bound with the minimum perturbation of the data. A review of the privacy-preserving transfer learning method is provided in section 3. A further application of conditionally deep autoencoders to inverse problem is considered in section 4. The reason being that a model related to the inverse problem is required, as discussed in section 5, for an analytical approximation of an information theoretic measure referred to as *information-leakage*. Section 5 presents the most important result of this study regarding variational approximation of information-leakage and development of a computational algorithm for calculating information-leakage. The significance of information-leakage assessment is due to the fact that the measures (for privacy-leakage, interpretability, and transferability), as defined in section 6, are in the form of information-leakages. The application of proposed measures to study the tradeoffs between TAI principles is demonstrated through the experiments made on the widely used MNIST digits dataset in section 8. Finally, the concluding remarks are provided in section 8.

2. A Review of Membership-Mappings Based Conditionally Deep Autoencoders

This section provides the review of membership-mappings and conditionally deep autoencoders from [10].

2.1. Notations

- Let $n, N, p, M \in \mathbb{N}$.
- Let $\mathcal{B}(\mathbb{R}^N)$ denote the *Borel σ -algebra* on \mathbb{R}^N , and let λ^N denote the *Lebesgue measure* on $\mathcal{B}(\mathbb{R}^N)$.
- Let $(\mathcal{X}, \mathcal{A}, \rho)$ be a probability space with unknown probability measure ρ .
- Let us denote by \mathcal{S} the set of finite samples of data points drawn i.i.d. from ρ , i.e.,

$$\mathcal{S} := \{(x^i \sim \rho)_{i=1}^N \mid N \in \mathbb{N}\}. \quad (1)$$

- $\mathbb{F}(\mathcal{X})$ denotes the set of \mathcal{A} - $\mathcal{B}(\mathbb{R})$ measurable functions $f : \mathcal{X} \rightarrow \mathbb{R}$, i.e.,

$$\mathbb{F}(\mathcal{X}) := \{f : \mathcal{X} \rightarrow \mathbb{R} \mid f \text{ is } \mathcal{A}\text{-}\mathcal{B}(\mathbb{R}) \text{ measurable}\}. \quad (2)$$

- For a sequence $\mathbf{x} = (x^1, \dots, x^N) \in \mathcal{S}$, let $|\mathbf{x}|$ denote the cardinality i.e. $|\mathbf{x}| = N$.
- If $\mathbf{x} = (x^1, \dots, x^N)$, $\mathbf{a} = (a^1, \dots, a^M) \in \mathcal{S}$, then $\mathbf{x} \wedge \mathbf{a}$ denotes the concatenation of the sequences \mathbf{x} and \mathbf{a} , i.e., $\mathbf{x} \wedge \mathbf{a} = (x^1, \dots, x^N, a^1, \dots, a^M)$.
- Let $\zeta_{\mathbf{x}} : \mathbb{R}^{|\mathbf{x}|} \rightarrow [0, 1]$ be a membership function satisfying the following properties:

Nowhere Vanishing: $\zeta_{\mathbf{x}}(\mathbf{y}) > 0$ for all $\mathbf{y} \in \mathbb{R}^{|\mathbf{x}|}$, i.e.,

$$\text{supp}[\zeta_{\mathbf{x}}] = \mathbb{R}^{|\mathbf{x}|}. \quad (3)$$

Positive and Bounded Integrals: the functions $\zeta_{\mathbf{x}}$ are absolutely continuous and Lebesgue integrable over the whole domain such that for all $\mathbf{x} \in \mathcal{S}$ we have

$$0 < \int_{\mathbb{R}^{|\mathbf{x}|}} \zeta_{\mathbf{x}} \, d\lambda^{|\mathbf{x}|} < \infty. \quad (4)$$

Consistency of Induced Probability Measure: the membership function induced probability measures $\mathbb{P}_{\zeta_{\mathbf{x}}}$, defined on any $A \in \mathcal{B}(\mathbb{R}^{|\mathbf{x}|})$, as

$$\mathbb{P}_{\zeta_{\mathbf{x}}}(A) := \frac{1}{\int_{\mathbb{R}^{|\mathbf{x}|}} \zeta_{\mathbf{x}} \, d\lambda^{|\mathbf{x}|}} \int_A \zeta_{\mathbf{x}} \, d\lambda^{|\mathbf{x}|} \quad (5)$$

are consistent in the sense that for all $\mathbf{x}, \mathbf{a} \in \mathcal{S}$:

$$\mathbb{P}_{\zeta_{\mathbf{x} \wedge \mathbf{a}}}(A \times \mathbb{R}^{|\mathbf{a}|}) = \mathbb{P}_{\zeta_{\mathbf{x}}}(A). \quad (6)$$

- Denote a collection of membership functions as

$$\Theta := \{\zeta_{\mathbf{x}} : \mathbb{R}^{|\mathbf{x}|} \rightarrow [0, 1] \mid (3), (4), (6), \mathbf{x} \in \mathcal{S}\}. \quad (7)$$

2.2. Student-t Membership-Mapping

Definition 1 (Student-t Membership-Mapping [10]). A Student-t membership-mapping, $\mathcal{F} \in \mathbb{F}(\mathcal{X})$, is a mapping with input space $\mathcal{X} = \mathbb{R}^n$ and a membership function $\zeta_x \in \Theta$ that is Student-t like:

$$\zeta_x(y) = \left(1 + 1/(\nu - 2)(y - m_y)^T K_{xx}^{-1}(y - m_y)\right)^{-\frac{\nu + |x|}{2}} \quad (8)$$

where $x \in \mathcal{S}$, $y \in \mathbb{R}^{|x|}$, $\nu \in \mathbb{R}_+ \setminus [0, 2]$ is the degrees of freedom, $m_y \in \mathbb{R}^{|x|}$ is the mean vector, and $K_{xx} \in \mathbb{R}^{|x| \times |x|}$ is the covariance matrix with its (i, j) -th element given as

$$(K_{xx})_{i,j} = kr(x^i, x^j) \quad (9)$$

where $kr : \mathbb{R}^n \times \mathbb{R}^n \rightarrow \mathbb{R}$ is a positive definite kernel function defined as

$$kr(x^i, x^j) = \sigma^2 \exp \left(-0.5 \sum_{k=1}^n w_k |x_k^i - x_k^j|^2 \right) \quad (10)$$

where x_k^i is the k -th element of x^i , σ^2 is the variance parameter, and $w = (w_1, \dots, w_n)$ with $w_k \geq 0$.

2.3. Interpolation by Student-t Membership-Mapping

Let $\mathcal{F} \in \mathbb{F}(\mathbb{R}^n)$ be a zero-mean Student-t membership-mapping. Let $x = \{x^i \in \mathbb{R}^n \mid i \in \{1, \dots, N\}\}$ be a given set of input points and the corresponding mapping outputs are represented by the vector $f := (\mathcal{F}(x^1), \dots, \mathcal{F}(x^N))$. Let $a = \{a^m \mid a^m \in \mathbb{R}^n, m \in \{1, \dots, M\}\}$ be the set of auxiliary inducing points and the mapping outputs corresponding to auxiliary inducing inputs, are represented by the vector $u := (\mathcal{F}(a^1), \dots, \mathcal{F}(a^M))$. It follows from [10] that f , based upon the interpolation on elements of u , could be represented by means of a membership function, $\mu_{f;u} : \mathbb{R}^N \rightarrow [0, 1]$, defined as

$$\mu_{f;u}(\tilde{f}) := \left(1 + \frac{(\tilde{f} - \bar{m}_f)^T \left(\frac{\nu + (u)^T (K_{aa})^{-1} u - 2}{\nu + M - 2} \bar{K}_{xx} \right)^{-1} (\tilde{f} - \bar{m}_f)}{\nu + M - 2} \right)^{-\frac{\nu + M + N}{2}} \quad (11)$$

$$\bar{m}_f = K_{xa}(K_{aa})^{-1}u \quad (12)$$

$$\bar{K}_{xx} = K_{xx} - K_{xa}(K_{aa})^{-1}K_{xa}^T. \quad (13)$$

Here, $K_{aa} \in \mathbb{R}^{M \times M}$ and $K_{xa} \in \mathbb{R}^{N \times M}$ are positive definite matrices with their (i, j) -th element given as

$$(K_{aa})_{i,j} = kr(a^i, a^j) \quad (14)$$

$$(K_{xa})_{i,j} = kr(x^i, a^j) \quad (15)$$

where $kr : \mathbb{R}^n \times \mathbb{R}^n \rightarrow \mathbb{R}$ is a positive definite kernel function defined as in (10).

The pair $(\mathbb{R}^N, \mu_{f;u})$ constitutes a fuzzy set and $\mu_{f;u}(\tilde{f})$ is interpreted as the degree to which \tilde{f} matches an attribute induced by f for a given u .

2.4. Variational Learning of a Membership-Mappings Based Model

2.4.1. A Modeling Scenario

Given a dataset $\{(x^i, y^i) \mid x^i \in \mathbb{R}^n, y^i \in \mathbb{R}^p, i \in \{1, \dots, N\}\}$, it is assumed that there exist zero-mean Student-t membership-mappings $\mathcal{F}_1, \dots, \mathcal{F}_p \in \mathbb{F}(\mathbb{R}^n)$ such that

$$y^i \approx [\mathcal{F}_1(x^i) \dots \mathcal{F}_p(x^i)]^T. \quad (16)$$

2.4.2. An Algorithm for Variational Learning of Membership-Mappings

Given the training data samples $\{(x^i, y^i) | i \in \{1, \dots, N\}\}$, an analytical solution has been derived in [10] for membership-mappings' learning under modeling scenario (16). Algorithm 1 outlines the various steps involved in the learning. With reference to Algorithm 1,

- y_j , for $j \in \{1, 2, \dots, p\}$, is defined as

$$y_j := [y_j^1 \ \dots \ y_j^N]^T \in \mathbb{R}^N \quad (17)$$

where y_j^i denotes the j -th element of y^i .

- ξ is given as

$$\xi = N\sigma^2. \quad (18)$$

- $\Psi \in \mathbb{R}^{N \times M}$ is a matrix with its (i, m) -th element given as

$$\Psi_{i,m} = \frac{\sigma^2}{\prod_{k=1}^n (\sqrt{1 + w_k \sigma_x^2})} \exp \left(-\frac{1}{2} \sum_{k=1}^n \frac{w_k |a_k^m - x_k^i|^2}{1 + w_k \sigma_x^2} \right) \quad (19)$$

where a_k^m and x_k^i denotes the k -th element of a^m and x^i respectively.

- $\Phi \in \mathbb{R}^{M \times M}$ is a matrix with its (m, m') -th element given as

$$\Phi_{m,m'} = \frac{\sigma^4}{\prod_{k=1}^n (\sqrt{1 + 2w_k \sigma_x^2})} \sum_{i=1}^N \exp \left(-\frac{1}{4} \sum_{k=1}^n w_k (a_k^m - a_k^{m'})^2 - \sum_{k=1}^n \frac{w_k |0.5(a_j^m + a_k^{m'}) - x_k^i|^2}{1 + 2w_k \sigma_x^2} \right). \quad (20)$$

- The quantities $(\hat{a}_\tau, \hat{b}_\tau, \hat{a}_z, \hat{b}_z, \hat{a}_r, \hat{b}_r, \hat{a}_s, \hat{b}_s)$ follow

$$\hat{a}_\tau = a_\tau + 0.5Np \quad (21)$$

$$\hat{b}_\tau(O) = b_\tau + \frac{\hat{a}_z}{2\hat{b}_z} O \quad (22)$$

$$\hat{a}_z = 1 + 0.5Np + \hat{a}_r/\hat{b}_r \quad (23)$$

$$\hat{b}_z(O) = \frac{\hat{a}_r}{\hat{b}_r} \frac{\hat{a}_s}{\hat{b}_s} + \frac{\hat{a}_\tau}{2\hat{b}_\tau} O \quad (24)$$

$$\hat{a}_r = a_r \quad (25)$$

$$\hat{b}_r = b_r + (\hat{a}_s/\hat{b}_s)(\hat{a}_z/\hat{b}_z) - \psi(\hat{a}_s) + \log(\hat{b}_s) - 1 - \psi(\hat{a}_z) + \log(\hat{b}_z) \quad (26)$$

$$\hat{a}_s = a_s + (\hat{a}_r/\hat{b}_r) \quad (27)$$

$$\hat{b}_s = b_s + (\hat{a}_r/\hat{b}_r)(\hat{a}_z/\hat{b}_z) \quad (28)$$

Algorithm 1 Variational learning of the membership-mappings [10]

Require: Dataset $\{(x^i, y^i) \mid x^i \in \mathbb{R}^n, y^i \in \mathbb{R}^p, i \in \{1, \dots, N\}\}$; number of auxiliary points $M \in \{1, 2, \dots, N\}$; the degrees of freedom associated to the Student-t membership-mapping $\nu \in \mathbb{R}_+ \setminus [0, 2]$.

- 1: Choose free parameters as $\sigma^2 = 1$ and $\sigma_x^2 = 0.01$.
- 2: The auxiliary inducing points are suggested to be chosen as the cluster centroids:

$$\mathbf{a} = \{a^m\}_{m=1}^M = \text{cluster_centroid}(\{x^i\}_{i=1}^N, M)$$

where $\text{cluster_centroid}(\{x^i\}_{i=1}^N, M)$ represents the k-means clustering on $\{x^i\}_{i=1}^N$.

- 3: Define $w = (w_1, w_2, \dots, w_n)$ such that w_k (for $k \in \{1, 2, \dots, n\}$) is equal to the inverse of squared-distance between two most-distant points in the set: $\{x_k^1, x_k^2, \dots, x_k^N\}$.
- 4: Compute K_{aa} , ξ , Ψ , and Φ using (14), (18), (19), and (20) respectively.
- 5: Choose $a_\tau = b_\tau = a_r = b_r = a_s = b_s = 1$.
- 6: Initialise $\hat{a}_\tau = \hat{b}_\tau = \hat{a}_z = \hat{b}_z = \hat{a}_r = \hat{b}_r = 1$.
- 7: Initialize \hat{a}_s and \hat{b}_s using (27) and (28).
- 8: **repeat**
- 9: Update $\mathcal{E}(\hat{m}_{u_j}(y_j))$ as

$$\mathcal{E}(\hat{m}_{u_j}(y_j)) = K_{aa} \left(\Phi + \frac{\xi - \text{Tr}((K_{aa})^{-1}\Phi)}{\nu + M - 2} K_{aa} + \frac{\hat{b}_\tau \hat{b}_z}{\hat{a}_\tau \hat{a}_z} K_{aa} \right)^{-1} (\Psi)^T y_j. \quad (29)$$

- 10: Update $\mathcal{E}(O)$ as

$$\begin{aligned} \mathcal{E}(O) = & \sum_{j=1}^p \left(\|y_j\|^2 - 2 (\mathcal{E}(\hat{m}_{u_j}(y_j)))^T (K_{aa})^{-1} (\Psi)^T y_j + (\mathcal{E}(\hat{m}_{u_j}(y_j)))^T (K_{aa})^{-1} \Phi (K_{aa})^{-1} \mathcal{E}(\hat{m}_{u_j}(y_j)) \right. \\ & \left. + (\mathcal{E}(\hat{m}_{u_j}(y_j)))^T \frac{\xi - \text{Tr}((K_{aa})^{-1}\Phi)}{\nu + M - 2} (K_{aa})^{-1} \mathcal{E}(\hat{m}_{u_j}(y_j)) \right). \end{aligned} \quad (30)$$

- 11: Update $\hat{a}_\tau, \hat{b}_\tau(\mathcal{E}(O)), \hat{a}_z, \hat{b}_z(\mathcal{E}(O)), \hat{a}_r, \hat{b}_r, \hat{a}_s, \hat{b}_s$ using (21), (22), (23), (24), (25), (26), (27), (28) respectively.
- 12: Estimate β as

$$\beta = (\hat{a}_\tau / \hat{b}_\tau)(\hat{a}_z / \hat{b}_z). \quad (31)$$

- 13: **until** (β nearly converges)
- 14: Compute matrix B as

$$B = \left(\Phi + \frac{\xi - \text{Tr}((K_{aa})^{-1}\Phi)}{\nu + M - 2} K_{aa} + \frac{\hat{b}_\tau \hat{b}_z}{\hat{a}_\tau \hat{a}_z} K_{aa} \right)^{-1} (\Psi)^T. \quad (32)$$

Compute matrix $\alpha = [\alpha_1 \ \dots \ \alpha_p]$ with its j -th column defined as

$$\alpha_j := \left(\Phi + \frac{\xi - \text{Tr}((K_{aa})^{-1}\Phi)}{\nu + M - 2} K_{aa} + \frac{\hat{b}_\tau \hat{b}_z}{\hat{a}_\tau \hat{a}_z} K_{aa} \right)^{-1} (\Psi)^T y_j \quad (33)$$

- 15: **return** The parameters set $\mathbb{M} = \{\alpha, w, \mathbf{a}, \sigma^2, \sigma_x^2, B\}$.
-

2.4.3. Prediction by Membership-Mappings

Given the parameters set $\mathbb{M} = \{\alpha, w, a, \sigma^2, \sigma_x^2, B\}$ returned by Algorithm 1, it follows from [10] that the learned membership-mappings could be used to predict output corresponding to any arbitrary input data point $x^* \in \mathbb{R}^n$ as

$$\hat{y}(x^*; \mathbb{M}) = \alpha^T (G(x^*; \mathbb{M}))^T. \quad (34)$$

Here, $G \in \mathbb{R}^{1 \times M}$ is a vector-valued function defined as

$$G(x; \mathbb{M}) := [G_1(x; \mathbb{M}) \cdots G_M(x; \mathbb{M})] \quad (35)$$

$$G_m(x; \mathbb{M}) := \frac{\sigma^2}{\prod_{k=1}^n (\sqrt{1 + w_k \sigma_x^2})} \exp \left(-\frac{1}{2} \sum_{k=1}^n \frac{w_k |a_k^m - x_k|^2}{1 + w_k \sigma_x^2} \right), \quad m \in \{1, \dots, M\}, \quad (36)$$

where a_k^m and x_k are the k -th elements of x and a^m respectively. Define for $i \in \{1, \dots, N\}$,

$$h^i(x; \mathbb{M}) := \sum_{m=1}^M (G_m(x; \mathbb{M})) (B)_{m,i} \quad (37)$$

where $(B)_{m,i}$ denotes the (m, i) -th element of B . Now, the prediction equation (34) could alternatively be expressed as

$$\hat{y}(x^*; \mathbb{M}) = h^1(x^*; \mathbb{M})y^1 + \cdots + h^N(x^*; \mathbb{M})y^N. \quad (38)$$

2.5. A Bregman Divergence Based Conditionally Deep Autoencoder

Definition 2 (Membership-Mapping Autoencoder [10]). A membership-mapping autoencoder, $\mathcal{G} : \mathbb{R}^p \rightarrow \mathbb{R}^p$, maps an input vector $y \in \mathbb{R}^p$ to $\mathcal{G}(y) \in \mathbb{R}^p$ such that

$$\mathcal{G}(y) \stackrel{\text{def}}{=} [\mathcal{F}_1(Py) \cdots \mathcal{F}_p(Py)]^T, \quad (39)$$

where \mathcal{F}_j ($j \in \{1, 2, \dots, p\}$) is a Student- t membership-mapping, $P \in \mathbb{R}^{n \times p}$ ($n \leq p$) is a matrix such that the product Py is a lower-dimensional encoding for y . That is, membership-mapping autoencoder first projects the input vector onto a lower dimensional subspace and then constructs the output vector through Student- t membership-mappings.

Definition 3 (Bregman divergence). The Bregman divergence \mathcal{B}_F , associated to a strictly convex twice differentiable function $F : \mathbb{R}^p \rightarrow \mathbb{R}$, is defined for any two vectors $y \in \mathbb{R}^p$ and $\hat{y} \in \mathbb{R}^p$ as

$$\mathcal{B}_F(\hat{y}, y) := F(\hat{y}) - F(y) - (\hat{y} - y)^T \nabla F(y) \quad (40)$$

where ∇F denotes the gradient of F . Different choices of F leads to different forms of Bregman divergences. We are in-particularly interested in the following two forms:

Bregman divergence associated to squared Euclidean norm: If we define $F(y) = (1/2)\|y\|^2$, then the corresponding Bregman divergence $\mathcal{B}_{sE}(\hat{y}, y)$ is defined as

$$\mathcal{B}_{sE}(\hat{y}, y) := \frac{1}{2} \|\hat{y} - y\|^2. \quad (41)$$

Relative entropy: For a vector $y = [y_1 \cdots y_p]^T$ (with $y_j > 0$ for all $j \in \{1, \dots, p\}$), if we define $F(y) = \sum_{j=1}^p (y_j \log(y_j) - y_j)$, then the Bregman divergence $\mathcal{B}_{re}(\hat{y}, y)$ is the unnormalized relative entropy:

$$\mathcal{B}_{re}(\hat{y}, y) := \sum_{j=1}^p \left(\hat{y}_j \log\left(\frac{\hat{y}_j}{y_j}\right) - \hat{y}_j + y_j \right). \quad (42)$$

Definition 4 (Conditionally Deep Autoencoder (CDA) [10]). A conditionally deep autoencoder, $\mathcal{D} : \mathbb{R}^p \rightarrow \mathbb{R}^p$, maps a vector $y \in \mathbb{R}^p$ to $\mathcal{D}(y) \in \mathbb{R}^p$ through a nested composition of finite number of membership-mapping autoencoders such that

$$\mathcal{D}(y) = \hat{y}^{l^*}, \quad (43)$$

$$\hat{y}^l = (\mathcal{G}_l \circ \dots \circ \mathcal{G}_2 \circ \mathcal{G}_1)(y), \quad \forall l \in \{1, 2, \dots, L\}, \quad (44)$$

$$l^* = \begin{cases} \arg \min_{l \in \{1, \dots, L\}} \mathcal{B}_{sE}(\hat{y}^l, y), & \text{choice 1} \\ \arg \min_{l \in \{1, \dots, L\}} \mathcal{B}_{re}([e^{\hat{y}_1^l} \dots e^{\hat{y}_p^l}]^T, [e^{y_1} \dots e^{y_p}]^T), & \text{choice 2} \end{cases} \quad (45)$$

where $\mathcal{G}_l(\cdot)$ is a membership-mapping autoencoder (Definition 2); \hat{y}^l is the output of l -th layer representing input vector y at certain abstraction level such that \hat{y}^1 is least abstract representation and \hat{y}^L is most abstract representation of the input vector; and the autoencoder output $\mathcal{D}(y)$ is equal to the output of the layer re-constructing the given input vector as good as possible where re-construction error is measured in-terms of Bregman divergence. The Bregman divergence could be chosen either of squared Euclidean norm form or of relative entropy form. The structure of deep autoencoder (as displayed in Fig. ??) is such that

$$\begin{aligned} \hat{y}^l &= \mathcal{G}_l(\hat{y}^{l-1}), \\ &= [\mathcal{F}_1^l(P^l \hat{y}^{l-1}) \dots \mathcal{F}_p^l(P^l \hat{y}^{l-1})]^T \end{aligned}$$

where $\hat{y}^0 = y$, $P^l \in \mathbb{R}^{n_l \times p}$ is a matrix with $n_l \in \{1, \dots, p\}$ such that $n_1 \geq n_2 \geq \dots \geq n_L$, and $\mathcal{F}_j^l(\cdot)$ is a Student- t membership-mapping.

2.5.1. Variational Learning Algorithm

Given a set of N samples $\{y^1, \dots, y^N\}$, Algorithm 2 is suggested for the variational learning of CDA.

Algorithm 2 Variational learning of conditionally deep autoencoder [10]

Require: Data set $\mathbf{Y} = \{y^i \in \mathbb{R}^p \mid i \in \{1, \dots, N\}\}$; the subspace dimension $n \in \{1, 2, \dots, p\}$; number of auxiliary points $M \in \{1, 2, \dots, N\}$; the number of layers $L \in \mathbb{Z}_+$.

- 1: Choose free parameters as $\nu^1 = 2.1, \nu^2 = \infty, \dots, \nu^L = \infty$.
- 2: **for** $l = 1$ to L **do**
- 3: Set subspace dimension associated to l -th layer as $n_l = \max(n - l + 1, 1)$.
- 4: Define $P^l \in \mathbb{R}^{n_l \times p}$ such that i -th row of P^l is equal to transpose of eigenvector corresponding to i -th largest eigenvalue of sample covariance matrix of data set \mathbf{Y} .
- 5: Define a latent variable $x^{l,i} \in \mathbb{R}^{n_l}$, for $i \in \{1, \dots, N\}$, as

$$x^{l,i} = \begin{cases} P^l y^i & \text{if } l = 1, \\ P^l \hat{y}^{l-1}(x^{l-1,i}; \mathbb{M}^{l-1}) & \text{if } l > 1 \end{cases} \quad (46)$$

where \hat{y}^{l-1} is the estimated output of the $(l-1)$ -th layer computed for the parameters set $\mathbb{M}^{l-1} = \{\alpha^{l-1}, w^{l-1}, a^{l-1}, \sigma^2, \sigma_x^2, B^{l-1}\}$.

- 6: Compute parameters set \mathbb{M}^l characterizing the membership-mappings associated to l -th layer by applying Algorithm 1 on data set $\{(x^{l,i}, y^i) \mid i \in \{1, \dots, N\}\}$ with number of auxiliary points M and degrees of freedom as ν^l .
 - 7: **end for**
 - 8: **return** The parameters set $\mathcal{M} = \{\{\mathbb{M}^1, \dots, \mathbb{M}^L\}, \{P^1, \dots, P^L\}\}$.
-

Definition 5 (Filtering by CDA [10]). Given a CDA with its parameters being represented by a set $\mathcal{M} = \{\{\mathbb{M}^1, \dots, \mathbb{M}^L\}, \{P^1, \dots, P^L\}\}$, the autoencoder can be applied for filtering a given input vector $y \in \mathbb{R}^p$ as follows:

$$x^l(y; \mathcal{M}) = \begin{cases} P^l y, & l = 1 \\ P^l \hat{y}^{l-1}(x^{l-1}; \mathbb{M}^{l-1}) & l \geq 2 \end{cases} \quad (47)$$

Here, \hat{y}^{l-1} is the output of the $(l-1)$ -th layer. Finally, CDA's output, $\mathcal{D}(y; \mathcal{M})$, is given as

$$\mathcal{D}(y; \mathcal{M}) = \hat{y}^{l^*}(x^{l^*}(y; \mathcal{M}); \mathbb{M}^{l^*}), \quad \text{where} \quad (48)$$

$$l^* = \begin{cases} \arg \min_{l \in \{1, \dots, L\}} \mathcal{B}_{sE}(\hat{y}^l(x^l(y; \mathcal{M}), \mathbb{M}^l), y), & \text{choice 1} \\ \arg \min_{l \in \{1, \dots, L\}} \mathcal{B}_{re}([e^{\hat{y}_1^l(x^l(y; \mathcal{M}), \mathbb{M}^l)} \dots e^{\hat{y}_p^l(x^l(y; \mathcal{M}), \mathbb{M}^l)}]^T, [e^{y_1} \dots e^{y_p}]^T), & \text{choice 2} \end{cases} \quad (49)$$

where \hat{y}_j^l denotes the j -th element of \hat{y}^l and \hat{y}^l is computed using (34) or equivalently (38). CDA's output could be expressed in-terms of training data samples using (38) as

$$\mathcal{D}(y; \mathcal{M}) = h^1(x^{l^*}(y; \mathcal{M}); \mathbb{M}^{l^*})y^1 + \dots + h^N(x^{l^*}(y; \mathcal{M}); \mathbb{M}^{l^*})y^N \quad (50)$$

where h^i is defined by (37).

2.5.2. A Wide Conditionally Deep Autoencoder

For a big dataset i.e. N is large, a wide conditionally deep autoencoder is defined as in Definition 6.

Definition 6 (A Wide CDA [10]). A wide CDA, $\mathcal{WD} : \mathbb{R}^p \rightarrow \mathbb{R}^p$, maps a vector $y \in \mathbb{R}^p$ to $\mathcal{WD}(y) \in \mathbb{R}^p$ through a parallel composition of S ($S \in \mathbb{Z}_+$) number of CDAs such that

$$\mathcal{WD}(y; \mathcal{P} = \{\mathcal{M}^s\}_{s=1}^S) = \mathcal{D}(y; \mathcal{M}^{s^*}), \text{ where} \quad (51)$$

$$s^* = \begin{cases} \arg \min_{s \in \{1, \dots, S\}} \mathcal{B}_{sE}(\mathcal{D}(y; \mathcal{M}^s), y), & \text{choice 1} \\ \arg \min_{s \in \{1, \dots, S\}} \mathcal{B}_{re}(\exp[\mathcal{D}(y; \mathcal{M}^s)], \exp[y]), & \text{choice 2} \end{cases} \quad (52)$$

Here, $\mathcal{D}(y; \mathcal{M}^s)$ denotes the output of s -th CDA (that was characterized by parameters set \mathcal{M}^s) and $\exp[\cdot]$ denotes the element-wise exponential.

Algorithm 3 is suggested for the variational learning of wide CDA.

Algorithm 3 Variational learning of wide CDA [10]

Require: Data set $\mathbf{Y} = \{y^i \in \mathbb{R}^p \mid i \in \{1, \dots, N\}\}$; the subspace dimension $n \in \{1, 2, \dots, p\}$; ratio $M/N \in (0, 1]$; the number of layers $L \in \mathbb{Z}_+$.

- 1: Apply k-means clustering to partition \mathbf{Y} into S subsets, $\{\mathbf{Y}^1, \dots, \mathbf{Y}^S\}$, where $S = \lceil N/1000 \rceil$.
 - 2: **for** $s = 1$ to S **do**
 - 3: Build a CDA, \mathcal{M}^s , by applying Algorithm 2 on \mathbf{Y}^s taking n as the subspace dimension; the number of auxiliary points as equal to $(M/N) \times \#\mathbf{Y}^s$ (where $\#\mathbf{Y}^s$ is the number of data points in \mathbf{Y}^s); and L as the number of layers.
 - 4: **end for**
 - 5: **return** the set of parameters sets: $\mathcal{P} = \{\mathcal{M}^s\}_{s=1}^S$.
-

2.6. Classification Applications

Definition 7 (A Classifier [10]). A classifier, $\mathcal{C} : \mathbb{R}^p \rightarrow \{1, 2, \dots, C\}$, maps a vector $y \in \mathbb{R}^p$ to $\mathcal{C}(y) \in \{1, 2, \dots, C\}$ such that

$$\mathcal{C}(y; \{\mathcal{P}_c\}_{c=1}^C) = \begin{cases} \arg \min_{c \in \{1, \dots, C\}} \mathcal{B}_{sE}(\mathcal{WD}(y; \mathcal{P}_c), y), & \text{choice 1} \\ \arg \min_{c \in \{1, \dots, C\}} \mathcal{B}_{re}(\exp[\mathcal{WD}(y; \mathcal{P}_c)], \exp[y]), & \text{choice 2} \end{cases} \quad (53)$$

where $\mathcal{WD}(y; \mathcal{P}_c)$, computed using (51), is the output of c -th wide CDA (that was characterized by parameters set \mathcal{P}_c) and $\exp[\cdot]$ denotes the element-wise exponential. The classifier assigns to an input vector the label of that class whose associated autoencoder best reconstructs the input vector where re-construction error is measured in-terms of Bregman divergence.

Algorithm 4 is provided for the learning of the classifier.

Algorithm 4 Variational learning of the classifier [10]

Require: Labeled data set $\mathbf{Y} = \{\mathbf{Y}_c \mid \mathbf{Y}_c = \{y^{i,c} \in \mathbb{R}^p \mid i \in \{1, \dots, N_c\}\}, c \in \{1, \dots, C\}\}$; the subspace dimension $n \in \{1, \dots, p\}$; ratio $M/N \in (0, 1]$; the number of layers $L \in \mathbb{Z}_+$.

- 1: **for** $c = 1$ to C **do**
 - 2: Build a wide CDA, $\mathcal{P}_c = \{\mathcal{M}_c^s\}_{s=1}^{S_c}$, by applying Algorithm 3 on \mathbf{Y}_c for given $n, M/N$, and L .
 - 3: **end for**
 - 4: **return** the set of parameters sets $\{\mathcal{P}_c\}_{c=1}^C$.
-

3. A Review of Privacy-Preserving Semi-Supervised Transfer Learning

This section reviews the method suggested in [7] for privacy-preserving semi-supervised transfer learning. The method of [7], with an adaptation to the current formulation of Bregman divergence based conditionally deep autoencoder, is described in the following:

Optimal noise adding mechanism for differentially private classifiers:. The approach suggested in [7] relies on a tailored noise adding mechanism to achieve a given level of differential privacy-loss bound with the minimum perturbation of the data. In particular, Algorithm 5 is suggested for a differentially private approximation of data samples and Algorithm 6 is suggested for building a differentially private classifier.

Algorithm 5 Differentially private approximation of data samples [7]

Require: Data set $\mathbf{Y} = \{y^i \in \mathbb{R}^p \mid i \in \{1, \dots, N\}\}$; differential privacy parameters: $d \in \mathbb{R}_+$, $\epsilon \in \mathbb{R}_+$, $\delta \in (0, 1)$.

- 1: A differentially private approximation of data samples is provided as

$$y_j^{+i} = y_j^i + F_{v_j^i}^{-1}(t_j^i; \epsilon, \delta, d), \quad t_j^i \in (0, 1) \quad (54)$$

where y_j^{+i} is j -th element of $y^{+i} \in \mathbb{R}^p$ and $F_{v_j^i}^{-1}$ is given as

$$F_{v_j^i}^{-1}(t_j^i; \epsilon, \delta, d) = \begin{cases} \frac{d}{\epsilon} \log\left(\frac{2t_j^i}{1-\delta}\right), & t_j^i < \frac{1-\delta}{2} \\ 0, & t_j^i \in [\frac{1-\delta}{2}, \frac{1+\delta}{2}] \\ -\frac{d}{\epsilon} \log\left(\frac{2(1-t_j^i)}{1-\delta}\right), & t_j^i > \frac{1+\delta}{2} \end{cases}, \quad t_j^i \in (0, 1). \quad (55)$$

- 2: **return** $\mathbf{Y}^+ = \{y^{+i} \in \mathbb{R}^p \mid i \in \{1, \dots, N\}\}$.
-

Algorithm 6 Variational learning of a differentially private classifier [7]

Require: Differentially private approximated dataset: $\mathbf{Y}^+ = \{\mathbf{Y}_c^+ \mid c \in \{1, \dots, C\}\}$; the subspace dimension $n \in \{1, \dots, p\}$; ratio $M/N \in (0, 1]$; the number of layers $L \in \mathbb{Z}_+$.

- 1: Run Algorithm 4 on \mathbf{Y}^+ to build a classifier characterized by parameters sets $\{\mathcal{P}_c^+\}_{c=1}^C$.
 - 2: **return** $\{\mathcal{P}_c^+\}_{c=1}^C$.
-

Semi-supervised learning scenario:. The aim is to transfer the knowledge extracted by a classifier trained using source dataset to the classifier of target domain such that privacy of source dataset is preserved. Let $\{\mathbf{Y}_c^{sr}\}_{c=1}^C$ be the labelled source dataset where $\mathbf{Y}_c^{sr} = \{y_{sr}^{i,c} \in \mathbb{R}^{p_{sr}} \mid i \in \{1, \dots, N_c^{sr}\}\}$ represents c -th labelled samples. The target dataset consist of a few labelled samples $\{\mathbf{Y}_c^{tg}\}_{c=1}^C$ (with $\mathbf{Y}_c^{tg} = \{y_{tg}^{i,c} \in \mathbb{R}^{p_{tg}} \mid i \in \{1, \dots, N_c^{tg}\}\}$) and another set of unlabelled samples $\mathbf{Y}_*^{tg} = \{y_{tg}^{i,*} \in \mathbb{R}^{p_{tg}} \mid i \in \{1, \dots, N_*^{tg}\}\}$.

Differentially private source domain classifier:. For a given differential privacy parameters: d, ϵ, δ ; Algorithm 5 is applied on \mathbf{Y}_c^{sr} to obtain the differentially private approximated data samples, $\mathbf{Y}_c^{+sr} = \{y_{sr}^{+i,c} \in \mathbb{R}^{p_{sr}} \mid i \in \{1, \dots, N_c^{sr}\}\}$, for all $c \in \{1, \dots, C\}$. Algorithm 6 is applied on $\{\mathbf{Y}_c^{+sr}\}_{c=1}^C$ to build a differentially private source domain classifier characterized by parameters sets $\{\mathcal{P}_c^{+sr}\}_{c=1}^C$.

Differentially private source domain latent subspace transformation-matrix:. For a lower-dimensional representation of both source and target samples, a subspace dimension, $n_{st} \in \{1, 2, \dots, \min(p_{sr}, p_{tg})\}$, is chosen. Let $V^{+sr} \in \mathbb{R}^{n_{st} \times p_{sr}}$ be the transformation-matrix with its i -th row equal to transpose of eigenvector corresponding to i -th largest eigenvalue of sample covariance matrix computed on $\{\mathbf{Y}_c^{+sr}\}_{c=1}^C$.

Differentially private class-centers in latent subspace of source domain:. Let $\bar{m}_c^{+sr} \in \mathbb{R}^{n_{st}}$ be the center of the c -th labelled noise added source data samples in latent subspace defined as

$$\bar{m}_c^{+sr} = \text{median} \left(\{V^{+sr} y_{sr}^{+i,c} \mid i \in \{1, \dots, N_c^{sr}\}\} \right). \quad (56)$$

Target domain latent subspace transformation-matrix:. Let $V^{tg} \in \mathbb{R}^{n_{st} \times p_{tg}}$ be the transformation-matrix with its i -th row equal to transpose of eigenvector corresponding to i -th largest eigenvalue of sample covariance matrix computed on $\{\mathbf{Y}_c^{tg}\}_{c=1}^C \cup \mathbf{Y}_*^{tg}$. For the case of homogeneous source and target domains (i.e. $p_{sr} = p_{tg}$), one could choose V^{tg} as equal to V^{+sr} .

Class-centers in latent subspace of target domain:. For a given classifier function, $\hat{c} : \mathbb{R}^{n_{st}} \rightarrow \{1, 2, \dots, C\}$, let $\bar{m}_c^{tg} \in \mathbb{R}^{n_{st}}$ be a vector defined as

$$\bar{m}_c^{tg} = \text{median} \left(\left\{ V^{tg} y_{tg}^{i,c} \mid i \in \{1, \dots, N_c^{tg}\} \right\} \cup \left\{ V^{tg} y_{tg}^{i,*} \mid \hat{c}(y_{tg}^{i,*}) = c, i \in \{1, \dots, N_*^{tg}\} \right\} \right) \quad (57)$$

A transformation for representing target data samples in source-data-space:. To represent a target sample in source-data-space, *subspace alignment* approach is followed. For a given set, $\theta = \{\bar{m}_c^{tg}, V^{tg}, \bar{m}_c^{+sr}, V^{+sr}\}$, a transformation, $f_c^{tg \rightarrow sr} : \mathbb{R}^{p_{tg}} \rightarrow \mathbb{R}^{p_{sr}}$, is defined as

$$f_c^{tg \rightarrow sr}(y_{tg}^{i,*}; \theta = \{\bar{m}_c^{tg}, V^{tg}, \bar{m}_c^{+sr}, V^{+sr}\}) := (V^{+sr})^T \left(V^{tg} y_{tg}^{i,*} - \bar{m}_c^{tg} + \bar{m}_c^{+sr} \right). \quad (58)$$

That is, $f_c^{tg \rightarrow sr}$ maps a target sample close to center of c -th labelled target data samples to a point in source-data-space that is close to center of c -th labelled source data samples.

A combination of source and target domain classifiers:. The label associated to $y_{tg}^{i,*}$ is predicted via combining both source and target domain classifiers as

$$\hat{c}(y_{tg}^{i,*}; \{\mathcal{P}_c^{tg}\}_{c=1}^C, \{\mathcal{P}_c^{+sr}\}_{c=1}^C, \theta) = \arg \min_{c \in \{1, \dots, C\}} \begin{cases} \min \left\{ \mathcal{B}_{sE} \left(\mathcal{WD}(y_{tg}^{i,*}; \mathcal{P}_c^{tg}), y_{tg}^{i,*} \right), \right. \\ \left. \mathcal{B}_{sE} \left(\mathcal{WD}(f_c^{tg \rightarrow sr}(y_{tg}^{i,*}; \theta); \mathcal{P}_c^{+sr}), f_c^{tg \rightarrow sr}(y_{tg}^{i,*}; \theta) \right) \right\}, & \text{choice 1} \\ \min \left\{ \mathcal{B}_{re} \left(\exp[\mathcal{WD}(y_{tg}^{i,*}; \mathcal{P}_c^{tg})], \exp[y_{tg}^{i,*}] \right), \right. \\ \left. \mathcal{B}_{re} \left(\exp[\mathcal{WD}(f_c^{tg \rightarrow sr}(y_{tg}^{i,*}; \theta); \mathcal{P}_c^{+sr})], \exp[f_c^{tg \rightarrow sr}(y_{tg}^{i,*}; \theta)] \right) \right\}, & \text{choice 2} \end{cases} \quad (59)$$

That is, $y_{tg}^{i,*}$ is assigned the c -th class label, if

- either the wide-deep autoencoder associated to c -th class of target data space (which is characterized by set of parameters \mathcal{P}_c^{tg}) could best reconstruct $y_{tg}^{i,*}$, or
- the differentially private wide-deep autoencoder associated to c -th class of source data space (which is characterized by set of parameters \mathcal{P}_c^{+sr}) could best reconstruct $f_c^{tg \rightarrow sr}(y_{tg}^{i,*}; \theta)$ (which is corresponding to $y_{tg}^{i,*}$ the transformed point in source data space close to the center of c -th labelled source data samples),

where the re-construction error is measured in-terms of Bregman divergence.

Building of target domain classifier:. The k -th iteration for building target domain classifier consists of following updates:

$$\{\mathcal{P}_c^{tg}|_k\}_{c=1}^C = \text{Algorithm 4} \left(\{\mathbf{Y}_c^{tg} \cup \mathbf{Y}_{*,c}^{tg}|_{k-1}\}_{c=1}^C, n|_k, (M/N)|_k, L \right) \quad (60)$$

$$\theta|_k = \{\bar{m}_c^{tg}|_{k-1}, V^{tg}, \bar{m}_c^{+sr}, V^{+sr}\} \quad (61)$$

$$\mathbf{Y}_{*,c}^{tg}|_k = \left\{ y_{tg}^{i,*} \mid \hat{c}(y_{tg}^{i,*}; \{\mathcal{P}_c^{tg}|_k\}_{c=1}^C, \{\mathcal{P}_c^{+sr}\}_{c=1}^C, \theta|_k) = c, i \in \{1, \dots, N_*^{tg}\} \right\} \quad (62)$$

$$\begin{aligned} \bar{m}_c^{tg}|_k &= \text{median} \left(\left\{ V^{tg} y_{tg}^{i,c} \mid i \in \{1, \dots, N_c^{tg}\} \right\} \right. \\ &\quad \left. \cup \left\{ V^{tg} y_{tg}^{i,*} \mid \hat{c}(y_{tg}^{i,*}; \{\mathcal{P}_c^{tg}|_k\}_{c=1}^C, \{\mathcal{P}_c^{+sr}\}_{c=1}^C, \theta|_k) = c, i \in \{1, \dots, N_*^{tg}\} \right\} \right) \end{aligned} \quad (63)$$

where $n|_k$ and $M/N|_k$ are parameters of Algorithm 4 in k -th iteration such that $\{n|_1, n|_2, \dots\}$ and $\{(M/N)|_1, (M/N)|_2, \dots\}$ are monotonically non-decreasing sequences. The reason for subspace dimension n and M/N ratio to follow a monotonically non-decreasing curve during the iterations is to use higher-level data features during initial iterations for updating the predicted-labels of unlabeled target data samples and as the number of iterations increases more and more lower-level data features are intended to be included in the process of updating the predicted-labels.

Algorithm 7 has been suggested for a practical implementation of the method.

4. Conditionally Deep Autoencoders for Inverse Problems

Given a CDA \mathcal{M} trained with dataset $\{y^i \in \mathbb{R}^p \mid i \in \{1, \dots, N\}\}$ using Algorithm 2, the CDA could be applied for solving the inverse problem related to $y = f_{t \rightarrow y}(t)$, where $f_{t \rightarrow y} : \mathbb{R}^q \rightarrow \mathbb{R}^p$ is a forward map. It follows from (50) that the CDA's output to any input y is given as

$$\mathcal{D}(y; \mathcal{M}) = \sum_{i=1}^N h^i \left(x^{l^*}(y; \mathcal{M}); \mathbb{M}^{l^*} \right) y^i. \quad (70)$$

Following the approach of [16], the deep autoencoder allows estimating t (where $y = f_{t \rightarrow y}(t)$) from y simply via replacing y^i by t^i (where $y^i = f_{t \rightarrow y}(t^i)$) in (70). That is, as

$$\hat{t}(y; \mathcal{M}, \{t^i\}_{i=1}^N) = \sum_{i=1}^N h^i \left(x^{l^*}(y; \mathcal{M}); \mathbb{M}^{l^*} \right) t^i. \quad (71)$$

The k -th element of \hat{t} is given as

$$\hat{t}_k(y; \mathcal{M}, \{t^i\}_{i=1}^N) = \sum_{i=1}^N h^i \left(x^{l^*}(y; \mathcal{M}); \mathbb{M}^{l^*} \right) t_k^i, \quad (72)$$

where t_k^i is k -th element of t^i and $k \in \{1, \dots, q\}$. Using (37) and (35), we have

$$\hat{t}_k(y; \mathcal{M}, \{t^i\}_{i=1}^N) = \left(G \left(x^{l^*}(y; \mathcal{M}); \mathbb{M}^{l^*} \right) \right) B \begin{bmatrix} t_k^1 & \dots & t_k^N \end{bmatrix}^T \quad (73)$$

For simplicity, define

$$\mathbf{m}_k = B \begin{bmatrix} t_k^1 & \dots & t_k^N \end{bmatrix}^T \quad (74)$$

$$g(y; \mathcal{M}) := G \left(x^{l^*}(y; \mathcal{M}); \mathbb{M}^{l^*} \right) \quad (75)$$

to express (73) as

$$\hat{t}_k(y; \mathcal{M}, \{t^i\}_{i=1}^N) = (g(y; \mathcal{M})) \mathbf{m}_k. \quad (76)$$

Algorithm 7 Differentially private semi-supervised transfer learning [7]

Require: A differentially private source domain classifier characterized by parameters sets $\{\mathcal{P}_c^{+sr}\}_{c=1}^C$; a differentially private source domain latent subspace transformation-matrix: $V^{+sr} \in \mathbb{R}^{n_{st} \times p_{sr}}$; the differentially private class-centers in latent subspace of source domain: $\{\bar{m}_c^{+sr} \in \mathbb{R}^{n_{st}}\}_{c=1}^C$; the set of a few labelled target samples: $\{\mathbf{Y}_c^{tg}\}_{c=1}^C$ (where $\mathbf{Y}_c^{tg} = \{y_{tg}^{i,c} \in \mathbb{R}^{p_{tg}} \mid i \in \{1, \dots, N_c^{tg}\}\}$ is the set of c -th labelled target samples); the set of unlabelled target samples: $\mathbf{Y}_*^{tg} = \{y_{tg}^{i,*} \in \mathbb{R}^{p_{tg}} \mid i \in \{1, \dots, N_*^{tg}\}\}$; a target domain initial classifier built using labelled target data samples and characterized by parameters sets: $\{\mathcal{P}_c^{tg}|_0\}_{c=1}^C$; the number of iterations: N_{it} ; a monotonically non-decreasing subspace dimension sequence: $\{n|_1, n|_2, \dots, n|_{N_{it}}\}$; a monotonically non-decreasing M/N ratio sequence: $\{(M/N)|_1, (M/N)|_2, \dots, (M/N)|_{N_{it}}\}$; the number of layers in the deep model associated to target domain classifier: L .

1: Use initial target classifier (i.e. $\{\mathcal{P}_c^{tg}|_0\}_{c=1}^C$) to predict class-labels of unlabelled target data samples and partition the total unlabelled samples into C different subsets such that each subset consists of samples with same predicted class label. That is, $\forall c \in \{1, 2, \dots, C\}$, build a subset:

$$\mathbf{Y}_{*,c}^{tg}|_0 = \left\{ y_{tg}^{i,*} \mid \mathcal{C}(y_{tg}^{i,*}; \{\mathcal{P}_c^{tg}|_0\}_{c=1}^C) = c, i \in \{1, \dots, N_*^{tg}\} \right\} \quad (64)$$

where $\mathcal{C}(\cdot)$ is defined by (53).

- 2: Define the target domain latent subspace transformation-matrix: $V^{tg} \in \mathbb{R}^{n_{st} \times p_{tg}}$ such that i -th row of V^{tg} is equal to transpose of eigenvector corresponding to i -th largest eigenvalue of sample covariance matrix computed on $\{\mathbf{Y}_c^{tg}\}_{c=1}^C \cup \mathbf{Y}_*^{tg}$. In the special case of $p_{sr} = p_{tg}$, V^{tg} could be defined as $V^{tg} = V^{+sr}$.
- 3: Initialize the center of the c -th labelled target data samples in latent subspace as

$$\begin{aligned} \bar{m}_c^{tg}|_0 &= \text{median} \left(\left\{ V^{tg} y_{tg}^{i,c} \mid i \in \{1, \dots, N_c^{tg}\} \right\} \right. \\ &\quad \left. \cup \left\{ V^{tg} y_{tg}^{i,*} \mid \mathcal{C}(y_{tg}^{i,*}; \{\mathcal{P}_c^{tg}|_0\}_{c=1}^C) = c, i \in \{1, \dots, N_*^{tg}\} \right\} \right) \end{aligned} \quad (65)$$

where $\mathcal{C}(\cdot)$ is defined by (53).

- 4: **for** $k = 1$ to N_{it} **do**
- 5: Set $L|_k = L$, if $k = N_{it}$, otherwise set $L|_k = 1$.
- 6: Update the target domain classifier as

$$\{\mathcal{P}_c^{tg}|_k\}_{c=1}^C = \text{Algorithm 4} \left(\left\{ \mathbf{Y}_c^{tg} \cup \mathbf{Y}_{*,c}^{tg}|_{k-1} \right\}_{c=1}^C, n|_k, (M/N)|_k, L|_k \right). \quad (66)$$

- 7: Estimate the class-labels for unlabelled target data samples using following:

$$\theta|_k = \{\bar{m}_c^{tg}|_{k-1}, V^{tg}, \bar{m}_c^{+sr}, V^{+sr}\} \quad (67)$$

$$\mathbf{Y}_{*,c}^{tg}|_k = \left\{ y_{tg}^{i,*} \mid \hat{\mathcal{C}}(y_{tg}^{i,*}; \{\mathcal{P}_c^{tg}|_k\}_{c=1}^C, \{\mathcal{P}_c^{+sr}\}_{c=1}^C, \theta|_k) = c, i \in \{1, \dots, N_*^{tg}\} \right\} \quad (68)$$

where $\hat{\mathcal{C}}(\cdot)$ is defined by (59).

- 8: Update the center of the c -th labelled target data samples in latent subspace as

$$\begin{aligned} \bar{m}_c^{tg}|_k &= \text{median} \left(\left\{ V^{tg} y_{tg}^{i,c} \mid i \in \{1, \dots, N_c^{tg}\} \right\} \right. \\ &\quad \left. \cup \left\{ V^{tg} y_{tg}^{i,*} \mid \hat{\mathcal{C}}(y_{tg}^{i,*}; \{\mathcal{P}_c^{tg}|_k\}_{c=1}^C, \{\mathcal{P}_c^{+sr}\}_{c=1}^C, \theta|_k) = c, i \in \{1, \dots, N_*^{tg}\} \right\} \right) \end{aligned} \quad (69)$$

where $\hat{\mathcal{C}}(\cdot)$ is defined by (59).

- 9: **end for**
- 10: **return** $\{\mathcal{P}_c^{tg}\}_{c=1}^C$, where $\mathcal{P}_c^{tg} = \mathcal{P}_c^{tg}|_{N_{it}}$.
-

4.1. A Prior Inverse Model

Expression (76) allows to estimate for any arbitrary y the corresponding t using CDA. This motivates introducing the following prior inverse model:

$$t_k = (g(y; \mathcal{M})) \theta_k + e_k \quad (77)$$

$$\theta_k \sim \mathcal{N}(\mathbf{m}_k, \Lambda_k^{-1}) \quad (78)$$

$$e_k \sim \mathcal{N}(0, \gamma^{-1}) \quad (79)$$

$$\gamma \sim \text{Gamma}(a_\gamma, b_\gamma) \quad (80)$$

where $k \in \{1, \dots, q\}$; $\mathcal{N}(\mathbf{m}_k, \Lambda_k^{-1})$ is the multivariate normal distribution with mean \mathbf{m}_k and covariance Λ_k^{-1} ; and $\text{Gamma}(a_\gamma, b_\gamma)$ is the Gamma distribution with shape parameter a_γ and rate parameter b_γ . The estimation provided by CDA (i.e. (76)) is incorporated by the prior model (77-80), since

$$\mathbb{E}[t_k] = \hat{t}_k(y; \mathcal{M}, \{t^i\}_{i=1}^N). \quad (81)$$

4.2. Variational Bayesian Inference of Inverse Model

Given the dataset, $\{(y^i \in \mathbb{R}^p, t^i \in \mathbb{R}^q) \mid i \in \{1, 2, \dots, N\}\}$, the variational Bayesian method is considered for an inference of the stochastic model (77), with priors as (78), (79), and (80). For all $i \in \{1, \dots, N\}$ and $k \in \{1, \dots, q\}$, we have

$$t_k^i = (g(y^i; \mathcal{M})) \theta_k + e_k^i, \quad (82)$$

where $\theta_k \sim \mathcal{N}(\mathbf{m}_k, \Lambda_k^{-1})$ and $e_k^i \sim \mathcal{N}(0, \gamma^{-1})$. Define $\mathbf{t}_k \in \mathbb{R}^N$, $\mathbf{e}_k \in \mathbb{R}^N$, and $R_y \in \mathbb{R}^{N \times M}$ as

$$\mathbf{t}_k = [t_k^1 \dots t_k^N]^T \quad (83)$$

$$\mathbf{e}_k = [e_k^1 \dots e_k^N]^T \quad (84)$$

$$R_y = \left[(g(y^1; \mathcal{M}))^T \dots (g(y^N; \mathcal{M}))^T \right]^T. \quad (85)$$

For all $k \in \{1, \dots, q\}$, we have

$$\mathbf{t}_k = R_y \theta_k + \mathbf{e}_k \quad (86)$$

$$p(\theta_k; \mathbf{m}_k, \Lambda_k) = \frac{\exp(-0.5(\theta_k - \mathbf{m}_k)^T \Lambda_k (\theta_k - \mathbf{m}_k))}{\sqrt{(2\pi)^M |(\Lambda_k)^{-1}|}} \quad (87)$$

$$p(\mathbf{e}_k; \gamma) = \frac{1}{\sqrt{(2\pi)^N (\gamma)^{-N}}} \exp(-0.5\gamma \|\mathbf{e}_k\|^2) \quad (88)$$

$$p(\gamma; a_\gamma, b_\gamma) = (b_\gamma^{a_\gamma} / \Gamma(a_\gamma)) (\gamma)^{a_\gamma-1} \exp(-b_\gamma \gamma). \quad (89)$$

Define the following sets:

$$\mathbf{t} := \{\mathbf{t}_1, \dots, \mathbf{t}_q\} \quad (90)$$

$$\theta := \{\theta_1, \dots, \theta_q\} \quad (91)$$

and consider the marginal probability of data \mathbf{t} which is given as

$$p(\mathbf{t}) = \int d\theta d\gamma p(\mathbf{t}, \theta, \gamma). \quad (92)$$

Let $q(\theta, \gamma)$ be an arbitrary distribution. The log marginal probability of \mathbf{t} can be expressed as

$$\log(p(\mathbf{t})) = \int d\theta d\gamma q(\theta, \gamma) \log(p(\mathbf{t})) \quad (93)$$

$$= \int d\theta d\gamma q(\theta, \gamma) \log\left(\frac{p(\mathbf{t}, \theta, \gamma)}{q(\theta, \gamma)}\right) + \int d\theta d\gamma q(\theta, \gamma) \log\left(\frac{q(\theta, \gamma)}{p(\theta, \gamma|\mathbf{t})}\right). \quad (94)$$

Define

$$\mathcal{L}(q(\theta, \gamma), \mathbf{t}) := \int d\theta d\gamma q(\theta, \gamma) \log(p(\mathbf{t}, \theta, \gamma)/q(\theta, \gamma)) \quad (95)$$

to express (94) as

$$\log(p(\mathbf{t})) = \mathcal{L}(q(\theta, \gamma), \mathbf{t}) + \text{KL}(q(\theta, \gamma) \| p(\theta, \gamma | \mathbf{t})) \quad (96)$$

where KL is the Kullback-Leibler divergence of $p(\theta, \gamma | \mathbf{t})$ from $q(\theta, \gamma)$ and \mathcal{L} , referred to as negative free energy, provides a lower bound on the the logarithmic evidence for the data.

The variational Bayesian approach minimizes the difference (in term of KL divergence) between variational and true posteriors via analytically maximizing negative free energy \mathcal{L} over variational distributions. However, the analytical derivation requires the following widely used mean-field approximation:

$$q(\theta, \gamma) = q(\theta)q(\gamma) \quad (97)$$

$$= q(\theta_1) \cdots q(\theta_q)q(\gamma). \quad (98)$$

Applying the standard variational optimization technique (as in [13, 15, 14, 11, 9, 12, 8]), it can be verified that the optimal variational distributions maximizing \mathcal{L} are as follows:

$$q^*(\theta_k) = \frac{\exp\left(-0.5(\theta_k - \hat{\mathbf{m}}_k)^T \hat{\Lambda}_k (\theta_k - \hat{\mathbf{m}}_k)\right)}{\sqrt{(2\pi)^M |(\hat{\Lambda}_k)^{-1}|}} \quad (99)$$

$$q^*(\gamma) = \left(\hat{b}_\gamma^{\hat{a}_\gamma} / \Gamma(\hat{a}_\gamma)\right) (\gamma)^{\hat{a}_\gamma - 1} \exp(-\hat{b}_\gamma \gamma) \quad (100)$$

where the parameters $(\hat{\Lambda}_k, \hat{\mathbf{m}}_k, \hat{a}_\gamma, \hat{b}_\gamma)$ satisfy the following:

$$\hat{\Lambda}_k = \Lambda_k + \left(\hat{a}_\gamma / \hat{b}_\gamma\right) (R_y)^T R_y \quad (101)$$

$$\hat{\mathbf{m}}_k = (\hat{\Lambda}_k)^{-1} \left(\Lambda_k \mathbf{m}_k + \left(\hat{a}_\gamma / \hat{b}_\gamma\right) (R_y)^T \mathbf{t}_k\right) \quad (102)$$

$$\hat{a}_\gamma = a_\gamma + 0.5qN \quad (103)$$

$$\hat{b}_\gamma = b_\gamma + 0.5 \sum_{k=1}^q \left\{ \|\mathbf{t}_k - R_y \hat{\mathbf{m}}_k\|^2 + \text{Tr} \left((\hat{\Lambda}_k)^{-1} (R_y)^T R_y \right) \right\}. \quad (104)$$

Algorithm 8 is suggested for variational Bayesian inference of the inverse model. The optimal distributions

Algorithm 8 Variational Bayesian inference of the inverse model

Require: Dataset $\{(y^i \in \mathbb{R}^p, t^i \in \mathbb{R}^q) \mid y^i = f_{t \rightarrow y}(t^i), i \in \{1, \dots, N\}\}$ and a CDA, \mathcal{M} , trained with dataset $\{y^i \in \mathbb{R}^p \mid i \in \{1, \dots, N\}\}$.

1: For all $k \in \{1, \dots, q\}$, compute \mathbf{m}_k using (74) taking $l = 1$ (i.e. first layer of DSFMA).

2: For all $k \in \{1, \dots, q\}$, choose $\Lambda_k = 10^{-6} I_M$.

3: Choose $a_\gamma = 10^{-6}$ and $b_\gamma = 10^{-6}$.

4: Initialise $\hat{a}_\gamma / \hat{b}_\gamma = 1$.

5: **repeat**

6: Update $\{\hat{\Lambda}_k, \hat{\mathbf{m}}_k \mid k \in \{1, \dots, q\}\}, \hat{a}_\gamma, \hat{b}_\gamma$ using (101), (102), (103), (104).

7: **until** (convergence **or** iterations = 1000)

8: **return** $\mathbb{M} = \{\{\hat{\mathbf{m}}_k, \hat{\Lambda}_k \mid k \in \{1, \dots, q\}\}, \hat{a}_\gamma, \hat{b}_\gamma\}$.

determined using Algorithm 8 define the so-called *Variational Bayesian Inverse Model (VBIM)* as stated in Remark 1.

Remark 1 (Variational Bayesian Inverse Model (VBIM)). The inverse mapping, $f_{t \rightarrow y}^{-1}$, is approximated as

$$t_k = (g(y; \mathcal{M})) \theta_k + e_k, \quad (105)$$

$$\theta_k \sim \mathcal{N}(\hat{\mathbf{m}}_k, \hat{\Lambda}_k^{-1}) \quad (106)$$

$$e_k \sim \mathcal{N}(0, \gamma^{-1}) \quad (107)$$

$$\gamma \sim \text{Gamma}(\hat{a}_\gamma, \hat{b}_\gamma) \quad (108)$$

where $k \in \{1, \dots, q\}$, x^l is defined by (47), l^* is given by (49), G is defined by (35), and $(\hat{\mathbf{m}}_k, \hat{\Lambda}_k, \hat{a}_\gamma, \hat{b}_\gamma)$ are returned by Algorithm 8.

Remark 2 (Estimation by VBIM). Given any y^* , the inverse model \mathbb{IM} (returned by Algorithm 8) can be used to estimate corresponding t^* (such that $y^* = f_{t \rightarrow y}(t^*)$) as

$$\tilde{t}(y^*; \mathcal{M}, \mathbb{IM}) = [\tilde{t}_1(y^*; \mathcal{M}, \mathbb{IM}) \cdots \tilde{t}_q(y^*; \mathcal{M}, \mathbb{IM})]^T \quad (109)$$

$$\tilde{t}_k(y^*; \mathcal{M}, \mathbb{IM}) = (g(y^*; \mathcal{M})) \hat{\mathbf{m}}_k, \forall k \in \{1, \dots, q\}. \quad (110)$$

5. Information-Leakage

Consider a scenario that $y = f_{t \rightarrow y}(t)$. The mutual information $I(t; y)$ measures the amount of information obtained about variable t through observing variable y . Given a scenario that $y = f_{t \rightarrow y}(t)$, the entropy $H(t)$ remains fixed independent of mapping $f_{t \rightarrow y}$ and thus the quantity $I(t; y) - H(t)$ is a measure of the amount of information about t leaked by the mapping $f_{t \rightarrow y}$. We define a measure of the amount of information about t leaked by the mapping $f_{t \rightarrow y}$ as

$$IL_{f_{t \rightarrow y}} := I(t; f_{t \rightarrow y}(t)) - H(t) \quad (111)$$

$$= I(t; y) - H(t). \quad (112)$$

The quantity $IL_{f_{t \rightarrow y}}$ is referred to as *information-leakage*. This section is dedicated to answer the question: *How to calculate without knowing data distributions the information-leakage?* Fig. 2 outlines a novel approach to the estimation of information-leakage. The approach consists of following steps:

1. A conditionally deep autoencoder (CDA), representing data features, induces a variational Bayesian inverse model (for approximating $f_{t \rightarrow y}^{-1}$), as explained in section 4.
2. It will be stated in subsection 5.1 that the inverse model facilitates deriving an analytical approximation of the mutual information between the two variables using variational optimization.
3. The analytical expression for mutual information and the available data samples can be used to compute information-leakage via an algorithm provided in subsection 5.2.

5.1. Variational Approximation of Mutual Information

There may be an interest in estimating the mutual information between a random variable t ($t \in \mathbb{R}^q$) and another random variable y ($y \in \mathbb{R}^p$), where the data distribution $p(t, y)$ is unknown. The mutual information between t and y is given as

$$I(t; y) = H(t) - H(t|y) \quad (113)$$

$$= H(t) + \int p(t, y) \log(p(t|y)) dt dy \quad (114)$$

$$= H(t) + \langle \log(p(t|y)) \rangle_{p(t, y)} \quad (115)$$

where $\langle g(y) \rangle_{p(y)}$ denotes the expectation of a function of random variable $g(y)$ w.r.t. probability density function $p(y)$; $H(t)$ and $H(t|y)$ are marginal and conditional entropies respectively. Consider the conditional probability of t which is given as

$$p(t|y) = \int d\theta d\gamma p(\theta, \gamma, t|y) \quad (116)$$

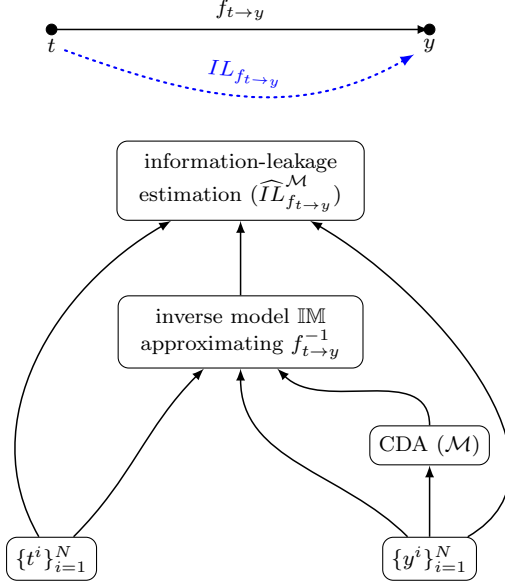


Figure 2: Information-leakage by a mapping $f_{t \rightarrow y}$, i.e. $IL_{f_{t \rightarrow y}}$, is evaluated via a variational approximation method based on a CDA (\mathcal{M}) induced inverse model \mathbb{M} .

where θ is a set defined as in (91). Let $q(\theta, \gamma)$ be an arbitrary distribution. The log conditional probability of t can be expressed as

$$\log(p(t|y)) = \int d\theta d\gamma q(\theta, \gamma) \log(p(t|y)) \quad (117)$$

$$= \int d\theta d\gamma q(\theta, \gamma) \log\left(\frac{p(\theta, \gamma, t|y)}{p(\theta, \gamma|t, y)}\right) \quad (118)$$

$$= \int d\theta d\gamma q(\theta, \gamma) \log(p(\theta, \gamma, t|y)/q(\theta, \gamma)) + \int d\alpha d\beta q(\theta, \gamma) \log\left(\frac{q(\theta, \gamma)}{p(\theta, \gamma|t, y)}\right). \quad (119)$$

Define

$$\mathcal{L}(q(\theta, \gamma), t, y) := \int d\theta d\gamma q(\theta, \gamma) \log\left(\frac{p(\theta, \gamma, t|y)}{q(\theta, \gamma)}\right) \quad (120)$$

to express (119) as

$$\log(p(t|y)) = \mathcal{L}(q(\theta, \gamma), t, y) + \text{KL}(q(\theta, \gamma) \| p(\theta, \gamma|t, y)) \quad (121)$$

where KL is Kullback-Leibler divergence of $p(\theta, \gamma|t, y)$ from $q(\theta, \gamma)$. Using (115),

$$I(t; y) = H(t) + \langle \mathcal{L}(q(\theta, \gamma), t, y) \rangle_{p(t, y)} + \langle \text{KL}(q(\theta, \gamma) \| p(\theta, \gamma|t, y)) \rangle_{p(t, y)}. \quad (122)$$

Since Kullback-Leibler divergence is always non-zero, it follows from (122) that $H(t) + \langle \mathcal{L} \rangle_{p(t, y)}$ provides a lower bound on $I(t; y)$ i.e.

$$I(t; y) \geq H(t) + \langle \mathcal{L}(q(\theta, \gamma), t, y) \rangle_{p(t, y)}. \quad (123)$$

Our approach to approximate $I(t; y)$ is to maximize its lower bound with respect to variational distribution $q(\theta, \gamma)$. That is, we solve

$$\hat{I}(t; y) = \max_{q(\theta, \gamma)} \left(H(t) + \langle \mathcal{L}(q(\theta, \gamma), t, y) \rangle_{p(t, y)} \right) \quad (124)$$

$$= H(t) + \max_{q(\theta, \gamma)} \langle \mathcal{L}(q(\theta, \gamma), t, y) \rangle_{p(t, y)}. \quad (125)$$

Result 1 (Variational Approximation of $I(t; y)$). Given the model (105)-(108), $\hat{I}(t; y)$ is given as

$$\begin{aligned} \hat{I}(t; y) = & H(t) - 0.5q \log(2\pi) + 0.5q \{F(\bar{a}_\gamma) - \log(\bar{b}_\gamma)\} \\ & - \frac{\bar{a}_\gamma}{2\bar{b}_\gamma} \sum_{k=1}^q \langle |t_k - g(y; \mathcal{M})\bar{\mathbf{m}}_k|^2 \rangle_{p(t, y)} - \frac{\bar{a}_\gamma}{2\bar{b}_\gamma} \sum_{k=1}^q \langle \text{Tr}((\bar{\Lambda}_k)^{-1}(g(y; \mathcal{M}))^T g(y; \mathcal{M})) \rangle_{p(y)} \\ & - \frac{1}{2} \sum_{k=1}^q \left\{ (\hat{\mathbf{m}}_k - \bar{\mathbf{m}}_k)^T \hat{\Lambda}_k (\hat{\mathbf{m}}_k - \bar{\mathbf{m}}_k) + \text{Tr}(\hat{\Lambda}_k (\bar{\Lambda}_k)^{-1}) - \log \left(\frac{|\bar{\Lambda}_k|^{-1}}{|\hat{\Lambda}_k|^{-1}} \right) \right\} + \frac{qM}{2} \\ & - \hat{a}_\gamma \log(\bar{b}_\gamma / \hat{b}_\gamma) + \log(\Gamma(\bar{a}_\gamma) / \Gamma(\hat{a}_\gamma)) - (\bar{a}_\gamma - \hat{a}_\gamma) \Psi(\bar{a}_\gamma) + (\bar{b}_\gamma - \hat{b}_\gamma) (\bar{a}_\gamma / \bar{b}_\gamma). \end{aligned} \quad (126)$$

Here, $F(\cdot)$ is the digamma function and the parameters $(\bar{\Lambda}_k, \bar{\mathbf{m}}_k, \bar{a}_\gamma, \bar{b}_\gamma)$ satisfy the following:

$$\bar{\Lambda}_k = \hat{\Lambda}_k + (\bar{a}_\gamma / \bar{b}_\gamma) \langle (g(y; \mathcal{M}))^T g(y; \mathcal{M}) \rangle_{p(y)} \quad (127)$$

$$\bar{\mathbf{m}}_k = (\bar{\Lambda}_k)^{-1} \left(\hat{\Lambda}_k \hat{\mathbf{m}}_k + \frac{\bar{a}_\gamma}{\bar{b}_\gamma} \langle (g(y; \mathcal{M}))^T t_k \rangle_{p(t, y)} \right) \quad (128)$$

$$\bar{a}_\gamma = \hat{a}_\gamma + 0.5q \quad (129)$$

$$\bar{b}_\gamma = \hat{b}_\gamma + \frac{1}{2} \sum_{k=1}^q \langle |t_k - g(y; \mathcal{M})\bar{\mathbf{m}}_k|^2 \rangle_{p(t, y)} + \frac{1}{2} \sum_{k=1}^q \langle \text{Tr}((\bar{\Lambda}_k)^{-1}(g(y; \mathcal{M}))^T g(y; \mathcal{M})) \rangle_{p(y)} \quad (130)$$

Proof: Consider

$$\mathcal{L}(q(\theta, \gamma), t, y) = \langle \log(p(t|\theta, \gamma, y)) \rangle_{q(\theta, \gamma)} + \langle \log(p(\theta, \gamma)/q(\theta, \gamma)) \rangle_{q(\theta, \gamma)}. \quad (131)$$

It follows from (105) and (107) that

$$\log(p(t_k|y, \theta_k, \gamma)) = -0.5 \log(2\pi) + 0.5 \log(\gamma) - 0.5\gamma |t_k - (g(y; \mathcal{M}))\theta_k|^2.$$

Since $t = [t_1 \ \cdots \ t_q]^T$, we have

$$\log(p(t|y, \theta, \gamma)) = -0.5q \log(2\pi) + 0.5q \log(\gamma) - 0.5\gamma \sum_{k=1}^q |t_k - (g(y; \mathcal{M}))\theta_k|^2. \quad (132)$$

Using (132) and (97-98) in (131), we have

$$\begin{aligned} \mathcal{L}(q(\theta, \gamma), t, y) = & -\frac{q}{2} \log(2\pi) + \frac{q}{2} \langle \log(\gamma) \rangle_{q(\gamma)} - \frac{\langle \gamma \rangle_{q(\gamma)}}{2} \sum_{k=1}^q \langle |t_k - (g(y; \mathcal{M}))\theta_k|^2 \rangle_{q(\theta_k)} \\ & + \sum_{k=1}^q \left\langle \log \left(\frac{p(\theta_k; \hat{\mathbf{m}}_k, \hat{\Lambda}_k)}{q(\theta_k)} \right) \right\rangle_{q(\theta_k)} + \left\langle \log \left(\frac{p(\gamma; a_\gamma, b_\gamma)}{q(\gamma)} \right) \right\rangle_{q(\gamma)}. \end{aligned} \quad (133)$$

$$\begin{aligned} \langle \mathcal{L}(q(\theta, \gamma), t, y) \rangle_{p(t, y)} = & -\frac{q}{2} \log(2\pi) + \frac{q}{2} \langle \log(\gamma) \rangle_{q(\gamma)} - \frac{\langle \gamma \rangle_{q(\gamma)}}{2} \sum_{k=1}^q \langle |t_k|^2 \rangle_{p(t)} \\ & - \frac{\langle \gamma \rangle_{q(\gamma)}}{2} \sum_{k=1}^q \left\langle (\theta_k)^T \langle (g(y; \mathcal{M}))^T g(y; \mathcal{M}) \rangle_{p(y)} \theta_k \right\rangle_{q(\theta_k)} \\ & + \langle \gamma \rangle_{q(\gamma)} \sum_{k=1}^q \left\langle (\theta_k)^T \langle (g(y; \mathcal{M}))^T t_k \rangle_{p(t, y)} \right\rangle_{q(\theta_k)} \\ & + \sum_{k=1}^q \left\langle \log \left(\frac{p(\theta_k; \hat{\mathbf{m}}_k, \hat{\Lambda}_k)}{q(\theta_k)} \right) \right\rangle_{q(\theta_k)} + \left\langle \log \left(\frac{p(\gamma; a_\gamma, b_\gamma)}{q(\gamma)} \right) \right\rangle_{q(\gamma)}. \end{aligned} \quad (134)$$

Now, $\langle \mathcal{L}(q(\theta, \gamma), t, y) \rangle_{p(t, y)}$ can be maximized w.r.t. $q(\theta_k)$ and $q(\gamma)$ using variational optimization. It can be seen that optimal distributions maximizing $\langle \mathcal{L}(q(\theta, \gamma), t, y) \rangle_{p(t, y)}$ are given as

$$q^*(\theta_k) = \frac{\exp(-0.5(\theta_k - \bar{m}_k)^T \bar{\Lambda}_k (\theta_k - \bar{m}_k))}{\sqrt{(2\pi)^M |(\bar{\Lambda}_k)^{-1}|}} \quad (135)$$

$$q^*(\gamma) = ((\bar{b}_\gamma)^{\bar{a}_\gamma} / \Gamma(\bar{a}_\gamma)) (\gamma)^{\bar{a}_\gamma - 1} \exp(-\bar{b}_\gamma \gamma) \quad (136)$$

where the parameters $(\bar{\Lambda}_k, \bar{m}_k, \bar{a}_\gamma, \bar{b}_\gamma)$ satisfy (127)-(130). The maximum attained value of $\langle \mathcal{L}(q(\theta, \gamma), t, y) \rangle_{p(t, y)}$ is given as

$$\begin{aligned} \max_{q(\theta, \gamma)} \langle \mathcal{L}(q(\theta, \gamma), t, y) \rangle_{p(t, y)} &= -0.5q \log(2\pi) + 0.5q \{F(\bar{a}_\gamma) - \log(\bar{b}_\gamma)\} \\ &\quad - \frac{1}{2} (\bar{a}_\gamma / \bar{b}_\gamma) \sum_{k=1}^q \langle |t_k - (g(y; \mathcal{M})) \bar{m}_k|^2 \rangle_{p(t, y)} \\ &\quad - \frac{\bar{a}_\gamma}{2\bar{b}_\gamma} \sum_{k=1}^q \langle \text{Tr}((\bar{\Lambda}_k)^{-1} (g(y; \mathcal{M}))^T g(y; \mathcal{M})) \rangle_{p(y)} \\ &\quad - \sum_{k=1}^q \text{KL}(q^*(\theta_k) \| p(\theta_k; \hat{m}_k, \hat{\Lambda}_k)) - \text{KL}(q^*(\gamma) \| p(\gamma; \hat{a}_\gamma, \hat{b}_\gamma)) \end{aligned}$$

where $F(\cdot)$ is the digamma function. After substituting the maximum value in (125) and calculating Kullback-Leibler divergences, we get (126). \blacksquare

5.2. Variational Approximation of Information-Leakage

The information theoretic measure $IL_{f_{t \rightarrow y}}$ could be estimated using available data samples based on Result 1. Algorithm 9 is stated for the variational approximation of the information-leakage. The information-leakage returned by Algorithm 9 has been denoted as $\widehat{IL}_{f_{t \rightarrow y}}^{\mathcal{M}}$ to emphasize that the information-leakage by the mapping $f_{t \rightarrow y}$ is estimated by means of a CDA \mathcal{M} .

Algorithm 9 Estimation of information-leakage, $IL_{f_{t \rightarrow y}} = I(t; y) - H(t)$, using variational approximation

Require: Dataset $\{(y^i \in \mathbb{R}^p, t^i \in \mathbb{R}^q) \mid y^i = f_{t \rightarrow y}(t^i), i \in \{1, \dots, N\}\}$ and a CDA, \mathcal{M} , trained with dataset $\{y^i \in \mathbb{R}^p \mid i \in \{1, \dots, N\}\}$.

- 1: Apply Algorithm 8 to obtain an inverse model $\mathbb{M} = \{\{\hat{m}_k, \hat{\Lambda}_k \mid k \in \{1, \dots, q\}\}, \hat{a}_\gamma, \hat{b}_\gamma\}$.
 - 2: Initialise $\bar{a}/\bar{b} = \hat{a}/\hat{b}$.
 - 3: **repeat**
 - 4: Update $\{\bar{\Lambda}_k, \bar{m}_k \mid k \in \{1, \dots, q\}\}, \bar{a}, \bar{b}$ using (127)-(130) where expectations $\langle \cdot \rangle_{p(x)}$ and $\langle \cdot \rangle_{p(t, x)}$ are approximated via sample-averages.
 - 5: **until** (convergence **or** iterations = 1000)
 - 6: Compute $\hat{I}(t; y) - H(t)$ using (126) where expectations $\langle \cdot \rangle_{p(y)}$ and $\langle \cdot \rangle_{p(t, y)}$ are approximated via sample-averages.
 - 7: Calculate $\widehat{IL}_{f_{t \rightarrow y}}^{\mathcal{M}} = \hat{I}(t; y) - H(t)$.
 - 8: **return** $\widehat{IL}_{f_{t \rightarrow y}}^{\mathcal{M}}$.
-

5.3. Verification of Information-Leakage Estimation Algorithm

To demonstrate the effectiveness of Algorithm 9 for estimating information-leakage, a scenario is generated where $t \in \mathbb{R}^{10}$ is Gaussian distributed such that $t \sim \mathcal{N}(0, 5I_{10})$, $y = t + \omega$, $\omega \sim \mathcal{N}(0, \sigma I_{10})$, and $\sigma \in [0.01, 5]$. Since the data distributions in this scenario are known, the information-leakage can be theoretically calculated and is given as

$$IL_{f_{t \rightarrow y}} = 5 \log(1 + 5/\sigma) - 0.5 \log(|(2\pi e 5 I_{10})|).$$

For a given value of $\sigma \in [0.01, 5]$, 1000 samples of t and y were simulated. A CDA was obtained using Algorithm 2 taking $n = 10$, $M = 500$, and $L = 1$. The CDA was then used in Algorithm 9 for estimating information-leakage. The experiments were carried out at different values of σ ranging from 0.01 to 5. Fig. 3 compares the plots of estimated and theoretically calculated values of information-leakage against σ .

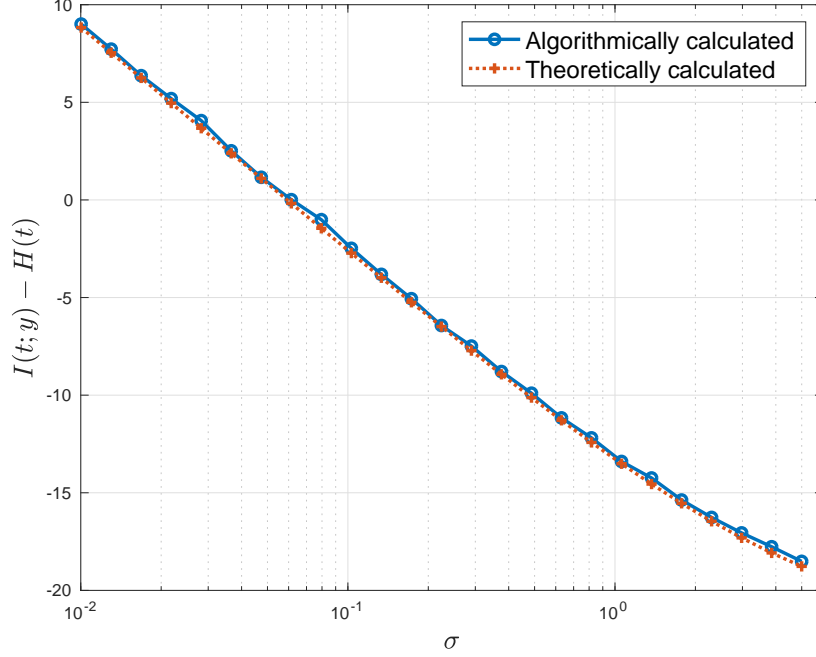


Figure 3: A comparison of the estimated information-leakage values with the theoretically calculated values.

A close agreement between the two plots in Fig. 3 verifies the effectiveness of Algorithm 9 in estimating information-leakage without knowing the data distributions.

6. Measures for Privacy-Leakage, Interpretability, and Transferability

This section defines information theoretic measures for privacy-leakage, interpretability, and transferability. For this, a few variables and mappings are introduced in Table 2.

Definition 8 (Privacy-Leakage). *Privacy-leakage (by the mapping from private variables to noise added feature vector) is a measure of the amount of information about private/sensitive variable x_{sr} leaked by the mapping $f_{x_{sr} \rightarrow y_{sr}^+}$ and is defined as*

$$IL_{f_{x_{sr} \rightarrow y_{sr}^+}} := I(x_{sr}; f_{x_{sr} \rightarrow y_{sr}^+}(x_{sr})) - H(x_{sr}) \quad (137)$$

$$= I(x_{sr}; y_{sr}^+) - H(x_{sr}). \quad (138)$$

Definition 9 (Interpretability-Measure). *Interpretability (of noise added feature vector) is measured as the amount of information about interpretable parameters t_{sr} leaked by the mapping $f_{t_{sr} \rightarrow y_{sr}^+}$ and is defined as*

$$IL_{f_{t_{sr} \rightarrow y_{sr}^+}} := I(t_{sr}; f_{t_{sr} \rightarrow y_{sr}^+}(t_{sr})) - H(t_{sr}) \quad (139)$$

$$= I(t_{sr}; y_{sr}^+) - H(t_{sr}). \quad (140)$$

Table 2: Introduced variables and mappings.

symbol/mapping	definition/meaning
$x_{sr} \in \mathbb{R}^{n_{sr}}$	vector representing private/sensitive variables associated to source domain
$y_{sr} \in \mathbb{R}^{p_{sr}}$	source domain feature vector
$t_{sr} \in \mathbb{R}^q$	vector representing the set of interpretable parameters associated to non-interpretable feature vector y_{sr}
$y_{sr}^+ \in \mathbb{R}^{p_{sr}}$	noise added feature vector (whose samples serve as training data for the learning of source model) obtained from y_{sr} via Algorithm 5
$f_{x_{sr} \rightarrow y_{sr}^+} : \mathbb{R}^{n_{sr}} \rightarrow \mathbb{R}^{p_{sr}}$	mapping from private variables to noise added feature vector, i.e., $y_{sr}^+ = f_{x_{sr} \rightarrow y_{sr}^+}(x_{sr})$
$f_{t_{sr} \rightarrow y_{sr}^+} : \mathbb{R}^q \rightarrow \mathbb{R}^{p_{sr}}$	mapping from interpretable parameters to non-interpretable noise added feature vector, i.e., $y_{sr}^+ = f_{t_{sr} \rightarrow y_{sr}^+}(t_{sr})$
$\{\mathcal{P}_c^{+sr}\}_{c=1}^C$	differentially private source domain autoencoders, representing data features of each of C classes, obtained via Algorithm 6
$y_{tg} \in \mathbb{R}^{p_{tg}}$	target domain feature vector
$\mathcal{L}_{tg} : \mathbb{R}^{p_{tg}} \rightarrow \{1, \dots, C\}$	mapping assigning ground-truth label to a target domain feature vector such that if $\mathcal{L}_{tg}(y_{tg}) = c$, then y_{tg} is labelled as c -th class
$f_{y_{tg} \rightarrow \hat{y}_{sr}}^{\mathcal{P}_1^{+sr}, \dots, \mathcal{P}_C^{+sr}} : \mathbb{R}^{p_{tg}} \rightarrow \mathbb{R}^{p_{sr}}$	transformation of y_{tg} to source domain and filtering through the autoencoder (that represents the source domain feature vectors of the same class as that of y_{tg}), i.e., $f_{y_{tg} \rightarrow \hat{y}_{sr}}^{\mathcal{P}_1^{+sr}, \dots, \mathcal{P}_C^{+sr}}(y_{tg}) = \mathcal{WD}\left(f_{\mathcal{L}_{tg}(y_{tg})}^{tg \rightarrow sr}(y_{tg}); \mathcal{P}_{\mathcal{L}_{tg}(y_{tg})}^{+sr}\right)$, where $f_c^{tg \rightarrow sr}$ (with $c = \mathcal{L}_{tg}(y_{tg})$) is defined by (58) and \mathcal{WD} represents the wide CDA (i.e. Definition 6)

Definition 10 (Transferability-Measure). *Transferability (from differentially private source domain data-representation models (i.e. $\mathcal{P}_1^{+sr}, \dots, \mathcal{P}_C^{+sr}$) to the target domain) is measured as the amount of information about target domain feature vector leaked by the mapping $f_{y_{tg} \rightarrow \hat{y}_{sr}}^{\mathcal{P}_1^{+sr}, \dots, \mathcal{P}_C^{+sr}}$ and is defined as*

$$IL_{f_{y_{tg} \rightarrow \hat{y}_{sr}}^{\mathcal{P}_1^{+sr}, \dots, \mathcal{P}_C^{+sr}}} := I\left(y_{tg}; f_{y_{tg} \rightarrow \hat{y}_{sr}}^{\mathcal{P}_1^{+sr}, \dots, \mathcal{P}_C^{+sr}}(y_{tg})\right) - H(y_{tg}). \quad (141)$$

The mapping $f_{y_{tg} \rightarrow \hat{y}_{sr}}^{\mathcal{P}_1^{+sr}, \dots, \mathcal{P}_C^{+sr}}$ transforms a target domain feature vector y_{tg} to the source domain followed by the filtering through the autoencoder (that represents the source domain feature vectors of the same class as that of y_{tg}), i.e.,

$$f_{y_{tg} \rightarrow \hat{y}_{sr}}^{\mathcal{P}_1^{+sr}, \dots, \mathcal{P}_C^{+sr}}(y_{tg}) = \mathcal{WD}\left(f_{\mathcal{L}_{tg}(y_{tg})}^{tg \rightarrow sr}(y_{tg}); \mathcal{P}_{\mathcal{L}_{tg}(y_{tg})}^{+sr}\right), \quad (142)$$

where $\mathcal{L}_{tg}(y_{tg}) \in \{1, \dots, C\}$, $f_c^{tg \rightarrow sr}$ is defined by (58), and \mathcal{WD} represents the wide CDA (i.e. Definition 6) characterized by $\mathcal{P}_{\mathcal{L}_{tg}(y_{tg})}^{+sr}$.

Definitions 8, 9, and 10 provide information theoretic measures for privacy-leakage, interpretability, and transferability. Since these measures are in the form of information-leakages, these measures can be calculated using Algorithm 9.

7. A Demonstrative Study

For demonstrating the application of the proposed measures (for privacy-leakage, interpretability, and transferability) to study the tradeoffs between TAI principles, experiments were made on the widely used MNIST digits dataset. The privacy-preserving interpretable and transferable learning method was implemented using MATLAB R2017b on a MacBook Pro machine with a 2.2 GHz Intel Core i7 processor and 16 GB of memory.

7.1. Data Preprocessing

The MNIST dataset contains 28×28 sized images divided into training set of 60000 images and testing set of 10000 images. The images' pixel values were divided by 255 to normalize the values in the range from 0 to 1. The 28×28 normalized pixel values of each image were flattened to an equivalent 784-dimensional data feature vector.

7.2. Interpretable Parameters

For MNIST digits dataset, there exist no additional interpretable parameters and thus we defined corresponding to a data feature vector $y \in \mathbb{R}^{784}$, an interpretable parameter vector $t \in \{0, 1\}^{10}$ such that j -th element $t_j = 1$, if j -th class-label is associated to y , otherwise $t_j = 0$. That is, interpretable vector t , in our experimental setting, represents the class-label assigned to data feature vector y .

7.3. Private Data

It was assumed that normalized pixel values are private, i.e., the vector representing private variables is equal to 784-dimensional data feature vector.

7.4. Semi-Supervised Transfer Learning Scenario

A transfer learning scenario was considered in the same setting as in [20, 7] where 60000 training samples constituted the source dataset; a set of 9000 test samples constituted target dataset, and the classification performance was evaluated on the remaining 1000 test samples. Out of 9000 target samples, only 10 samples per class were labelled and rest 8900 target samples remained as unlabelled.

7.5. Source Domain Noise Adding Mechanism Settings

Algorithm 5 is applied with $d = 1$ to obtain the differentially private approximations of source dataset at different values of privacy-loss bound $\epsilon \in \{0.1, 1, 2, 8, \infty\}$ while keeping failure probability fixed at $\delta = 1e-5$.

7.6. Transfer Learning Algorithm Settings

Following [7], the inputs required by Algorithm 7 are obtained as described below:

1. Differentially private source domain classifier is built using Algorithm 6 taking subspace dimension as equal to $\min(20, p_{sr})$ (where p_{sr} is the dimension of source data samples), ratio M/N as equal to 0.5, and number of layers as equal to 5.
2. Differentially private source domain latent subspace transformation-matrix is computed with $n_{st} = \min(\lceil p_{sr}/2 \rceil, p_{tg})$, where p_{tg} is the dimension of target data samples.
3. Differentially private class-centers in latent subspace of source domain are computed using (56).
4. Initial target domain classifier is built using Algorithm 4 on labelled target samples taking subspace dimension as equal to $\min(20, \min_{1 \leq c \leq C} \{N_c^{tg}\} - 1)$ (where N_c^{tg} is the number of c -th class labelled target samples), ratio M/N as equal to 1, and number of layers as equal to 1.
5. The number of iterations is set equal to 4; the monotonically non-decreasing subspace dimension sequence is chosen as $\{4, 6, 8, 10\}$; the monotonically non-decreasing M/N ratio sequence is chosen as $\{\frac{1}{10}, \frac{1}{8}, \frac{1}{6}, \frac{1}{4}\}$.
6. The number of layers in the deep model associated to target domain classifier is set as equal to 5.

7.7. Information-Leakage Estimation Algorithm Settings

The CDA required by Algorithm 9 for calculating information-leakage is obtained using Algorithm 2 taking $n = 20$, $M = \lceil N/10 \rceil$, and $L = 1$.

7.8. Experimental Design

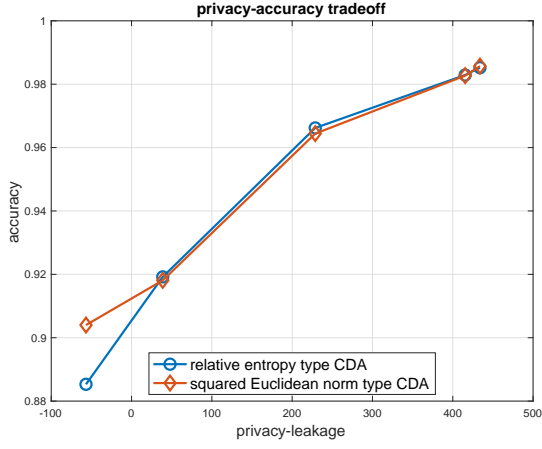
10 independent experiments were made where in each experiment, the test samples, target samples, and target labelled samples were chosen randomly. Each of 10 experiments involves 5 different privacy-preserving transfer learning scenarios with privacy-loss bound values as $\epsilon = \infty$ (i.e. non-private), $\epsilon = 8$, $\epsilon = 2$, $\epsilon = 1$, and $\epsilon = 0.1$. In each scenario, privacy-leakage (i.e. Definition 8) and interpretability-measure (i.e. Definition 9) were calculated via applying Algorithm 9 on 100 per class randomly chosen source domain samples while transferability-measure (i.e. Definition 10) was calculated via applying Algorithm 9 on labelled target samples. Further, for each scenario, the results are obtained for both choices of Bregman divergence (i.e. squared Euclidean norm and relative entropy).

7.9. Results

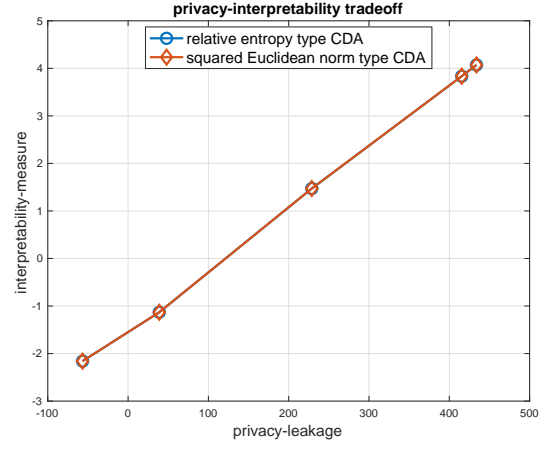
The averaged results over 10 independent experiments have been reported in Table 3 and plotted in Fig. 4. Fig. 4(a), Fig. 4(b), and Fig. 4(c) display the privacy-accuracy tradeoff curve, privacy-interpretability tradeoff curve, and privacy-transferability tradeoff curve respectively. As expected and observed in Fig. 4(f), the transferability-measure is positively correlated with the classification accuracy on target test samples. Since we have defined the interpretable vector associated to a feature vector as representing the class-label, the positive correlations of interpretability-measure with the accuracy and the transferability-measure are observed in Fig. 4(e) and Fig. 4(d) respectively.

Table 3: Results of experiments on MNIST dataset for evaluating privacy-leakage, interpretability, and transferability.

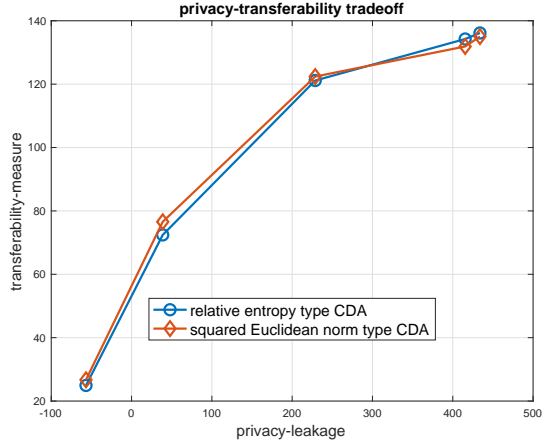
CDA type	Privacy -Leakage	Interpretability -Measure	Transferability -Measure	Accuracy
relative entropy	433.8497	4.0714	136.1498	0.9852
	415.4332	3.8345	134.2483	0.9829
	228.7308	1.4717	121.1469	0.9662
	38.8434	-1.1309	72.4297	0.9192
	-56.7136	-2.1589	24.9260	0.8853
squared Euclidean norm	433.8497	4.0714	135.0105	0.9857
	415.4332	3.8345	131.8903	0.9827
	228.7308	1.4717	122.3949	0.9644
	38.8434	-1.1309	76.5772	0.9181
	-56.7136	-2.1589	26.7081	0.9040



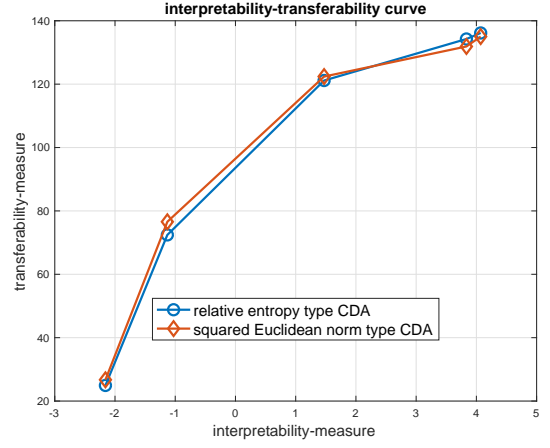
(a) privacy-leakage vs. accuracy



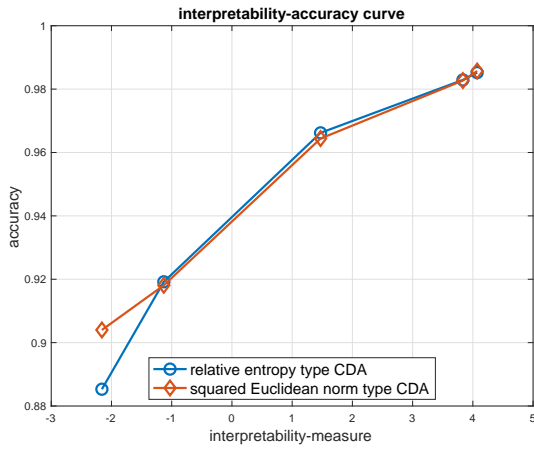
(b) privacy-leakage vs. interpretability-measure



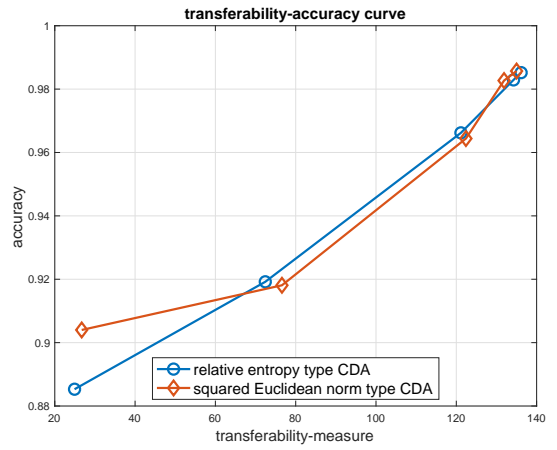
(c) privacy-leakage vs. transferability-measure



(d) interpretability-measure vs. transferability-measure



(e) interpretability-measure vs. accuracy



(f) transferability-measure vs. accuracy

Figure 4: The plots between privacy-leakage, interpretability-measure, transferability-measure, and accuracy for MNIST dataset.

7.10. Visualization Examples

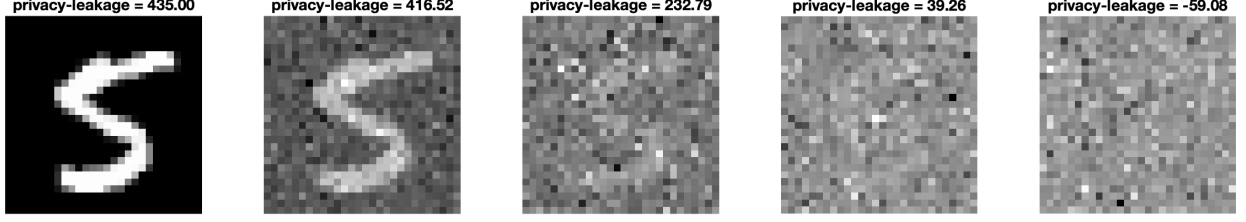


Figure 5: An example of a source domain sample corresponding to different levels of privacy-leakage. While moving from left to right in the figure, the privacy-leakage decreases as 435, 416.52, 232.79, 39.26, -59.08.

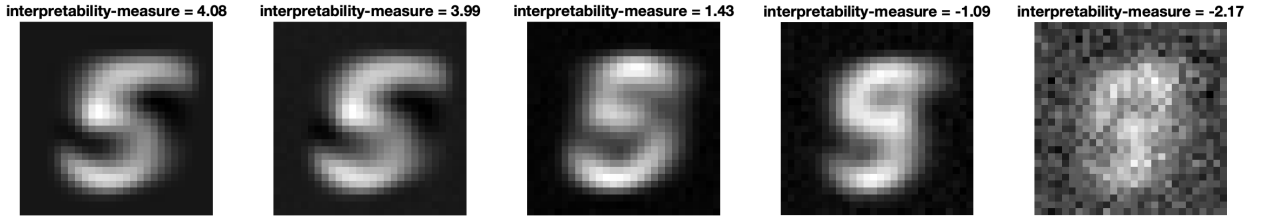


Figure 6: An example of a source domain sample corresponding to different levels of interpretability-measure. While moving from left to right in the figure, the interpretability-measure decreases as 4.08, 3.99, 1.43, -1.09, -2.17.

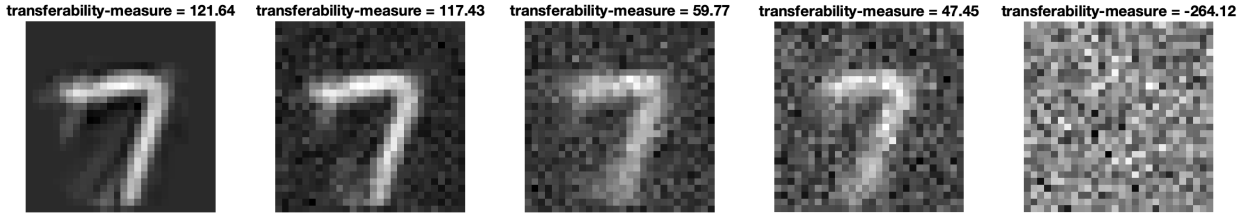


Figure 7: An example of a target domain sample transformed, via (142), to the source domain corresponding to different levels of transferability-measure. While moving from left to right in the figure, the transferability-measure decreases as 121.64, 117.43, 59.77, 47.45, -264.12.

Fig. 5 visualizes the level of noise to be added to the data feature samples for different values of privacy-leakage. For a visualization of the interpretability-measure, the interpretable parameters associated to a feature vector can be estimated by the inverse model (as stated in Remark 2). Since the interpretable parameters represent in this case a class-label, the estimated interpretable vector $\tilde{t} \in \mathbb{R}^{10}$ is transformed, for a visualization, to the pixel-domain as $\tilde{t}_1 \bar{y}_{sr}^{+1} + \dots + \tilde{t}_{10} \bar{y}_{sr}^{+10}$, where \tilde{t}_c is c -th element of \tilde{t} and \bar{y}_{sr}^{+c} is the mean of all c -th labelled noise added source data samples. Fig. 6 visualizes the different levels of interpretability via transforming estimated interpretable parameters to the pixel-domain. Finally, the different levels of transferability are visualized in Fig. 7 via transforming a target domain sample to the source domain using (142).

8. Concluding Remarks

The paper has introduced an information theoretic trustworthy AI framework. The information theoretic measures have been defined for privacy-leakage, interpretability, and transferability to study the inherent tradeoffs between TAI principles. This is the first study to develop information theory based unified approach to trustworthy AI. Although the text has not focused on federated and distributed learning, the transfer learning approach could be easily extended to the multi-party system and the transferability-measure could be calculated for any pair of parties. Also, the explainability of the conditionally deep autoencoders follows, similar to as in [16], via estimating interpretable parameters from non-interpretable data feature vectors using variational Bayesian inverse model (see, Remark 2). Further, the inverse model (stated in Remark 1) quantifies uncertainties on the estimation of parameters (of interest) which is also important for a user’s trust on the model. The proposed unified approach to privacy-preserving interpretable and transferable learning involves Bregman divergence based conditionally deep autoencoders, albeit other data representation learning models could be explored under the proposed trustworthy AI framework.

References

- [1] Floridi, L., 2019. Establishing the rules for building trustworthy ai. *Nature Machine Intelligence* 1, 261–262. URL: <https://doi.org/10.1038/s42256-019-0055-y>, doi:10.1038/s42256-019-0055-y.
- [2] Floridi, L., Cows, J., 2019. A unified framework of five principles for ai in society. *Harvard Data Science Review* 1. URL: <https://hdsr.mitpress.mit.edu/pub/10jsh9d1>, doi:10.1162/99608f92.8cd550d1. <https://hdsr.mitpress.mit.edu/pub/10jsh9d1>.
- [3] Floridi, L., Cows, J., Beltrametti, M., Chatila, R., Chazerand, P., Dignum, V., Luetge, C., Madelin, R., Pagallo, U., Rossi, F., Schafer, B., Valcke, P., Vayena, E., 2018. Ai4people—an ethical framework for a good ai society: Opportunities, risks, principles, and recommendations. *Minds and Machines* 28, 689–707. URL: <https://doi.org/10.1007/s11023-018-9482-5>, doi:10.1007/s11023-018-9482-5.
- [4] Future of Life Institute, 2017. Asilomar AI Principles. <https://futureoflife.org/ai-principles/>.
- [5] Hagendorff, T., 2020. The ethics of ai ethics: An evaluation of guidelines. *Minds and Machines* 30, 99–120. URL: <https://doi.org/10.1007/s11023-020-09517-8>, doi:10.1007/s11023-020-09517-8.
- [6] High-Level Expert Group on AI, 2019. Ethics guidelines for trustworthy AI. Report. European Commission. Brussels. URL: <https://ec.europa.eu/digital-single-market/en/news/ethics-guidelines-trustworthy-ai>.
- [7] Kumar, M., 2021. Differentially private transfer learning with conditionally deep autoencoders. <https://arxiv.org/abs/2105.04615>. arXiv:2105.04615.
- [8] Kumar, M., Brunner, D., Moser, B.A., Freudenthaler, B., 2020. Variational optimization of informational privacy, in: Kotsis, G., Tjoa, A.M., Khalil, I., Fischer, L., Moser, B., Mashkoor, A., Sametinger, J., Fensel, A., Martinez-Gil, J. (Eds.), *Database and Expert Systems Applications*, Springer International Publishing, Cham. pp. 32–47.
- [9] Kumar, M., Insan, A., Stoll, N., Thurow, K., Stoll, R., 2016. Stochastic fuzzy modeling for ear imaging based child identification. *IEEE Transactions on Systems, Man, and Cybernetics: Systems* 46, 1265–1278. doi:10.1109/TSMC.2015.2468195.
- [10] Kumar, M., Moser, B.A., Fischer, L., Freudenthaler, B., 2021a. Membership-mappings for data representation learning. <https://arxiv.org/abs/2104.07060>. arXiv:2104.07060.
- [11] Kumar, M., Neubert, S., Behrendt, S., Rieger, A., Weippert, M., Stoll, N., Thurow, K., Stoll, R., 2012. Stress monitoring based on stochastic fuzzy analysis of heartbeat intervals. *IEEE Transactions on Fuzzy Systems* 20, 746–759. doi:10.1109/TFUZZ.2012.2183602.
- [12] Kumar, M., Rossbory, M., Moser, B.A., Freudenthaler, B., 2021b. An optimal (ϵ, δ) -differentially private learning of distributed deep fuzzy models. *Information Sciences* 546, 87 – 120. URL: <http://www.sciencedirect.com/science/article/pii/S0020025520307106>, doi:<https://doi.org/10.1016/j.ins.2020.07.044>.
- [13] Kumar, M., Stoll, N., Stoll, R., 2010. Variational bayes for a mixed stochastic/deterministic fuzzy filter. *IEEE Transactions on Fuzzy Systems* 18, 787–801. doi:10.1109/TFUZZ.2010.2048331.
- [14] Kumar, M., Stoll, N., Stoll, R., 2011. Stationary Fuzzy Fokker-Planck Learning and Stochastic Fuzzy Filtering. *IEEE Transactions on Fuzzy Systems* 19, 873–889. doi:10.1109/TFUZZ.2011.2148724.
- [15] Kumar, M., Stoll, N., Stoll, R., Thurow, K., 2016. A Stochastic Framework for Robust Fuzzy Filtering and Analysis of Signals-Part I. *IEEE Transactions on Cybernetics* 46, 1118–1131. doi:10.1109/TCYB.2015.2423657.
- [16] Kumar, M., Zhang, W., Weippert, M., Freudenthaler, B., 2020. An explainable fuzzy theoretic nonparametric deep model for stress assessment using heartbeat intervals analysis. *IEEE Transactions on Fuzzy Systems* , 1–1doi:10.1109/TFUZZ.2020.3029284.
- [17] Mcknight, D.H., Carter, M., Thatcher, J.B., Clay, P.F., 2011. Trust in a specific technology: An investigation of its components and measures. *ACM Trans. Manage. Inf. Syst.* 2. doi:10.1145/1985347.1985353.
- [18] for the New Generation Artificial Intelligence, C.N.G.C., 2019. Governance principles for the new generation artificial intelligence—developing responsible artificial intelligence. <https://www.chinadaily.com.cn/a/201906/17/WS5d07486ba3103dbf14328ab7.html>.

- [19] OECD, 2019. Oecd principles on ai. <https://www.oecd.org/going-digital/ai/principles/>.
- [20] Papernot, N., Abadi, M., Erlingsson, ., Goodfellow, I.J., Talwar, K., 2017. Semi-supervised knowledge transfer for deep learning from private training data., in: ICLR, OpenReview.net. URL: <http://dblp.uni-trier.de/db/conf/iclr/iclr2017.html#PapernotAEGT17>.
- [21] Thiebes, S., Lins, S., Sunyaev, A., 2020. Trustworthy artificial intelligence. Electronic Markets doi:10.1007/s12525-020-00441-4.
- [22] UK House of Lords, 2017. Ai in the uk: ready, willing and able? <https://publications.parliament.uk/pa/ld201719/ldselect/ldai/100/100.htm>.
- [23] Université de Montréal, 2017. Montreal declaration for a responsible development of ai. <https://www.montrealdeclaration-responsibleai.com/the-declaration>.
- [24] Vought, R.T., 2020. Guidance for regulation of artificial intelligence applications. <https://www.whitehouse.gov/wp-content/uploads/2020/01/Draft-OMB-Memo-on-Regulation-of-AI-1-7-19.pdf>.